BINARY KERNEL METHOD IN CLASSICAL STATISTICAL MECHANICS

by

JAMES F. LIND

A dissertation submitted to the Graduate Faculty in Chemistry in partial fulfillment of the requirements for the degree of Doctor of Philosophy, The City University of New York

1974

This manuscript has been read and accepted for the Graduate Faculty in Chemistry in satisfaction of the dissertation requirement for the degree of Doctor of Philosophy.

19 April 1974
date

Charles E. Hecht
Professor Charles E. Hecht, Chairman of Examining Committee

4/18/74
date

Leonard H. Schwartz
Professor Leonard H. Schwartz, Executive Officer

Vojtech Fried
Professor Vojtech Fried

Ira N. Levine
Professor Ira N. Levine

L. M. Massa
Professor Louis Massa

Supervisory Committee

The City University of New York

Abstract

BINARY KERNEL METHOD IN CLASSICAL

STATISTICAL MECHANICS

BY

JAMES F. LIND

Advisor: Professor Charles E. Hecht

The binary kernel expansion method was developed by T.D. Lee and C.N. Yang to study the effects of interactions among the particles of quantum mechanical systems. This method involves use of Lee-Yang diagrams to represent the interactions as an expansion in powers of the binary kernel function. This binary kernel function can be found from knowledge of how two particles interact. For a system of ℓ particles the binary kernel expansion begins with the $(\ell - 1)$st power of the binary kernel function and involves successively higher powers of it. An expansion of the binary kernel function developed by Lee and Yang allowed use of only the lowest and next-to-lowest powers of it in applying the method to the Bose-Einstein gas at very low temperatures.

The aim of this work was to adapt this binary kernel method to systems obeying classical mechanics. It was found that in the classical limit the Lee-Yang binary kernel expansion converges to the Mayer cluster expansion for classical systems only if all powers of

the binary kernel function are included in the expansion. If only a finite number of terms are considered the correct classical results are not obtained. This is demonstrated explicitly for the cases of three and four particle systems interacting as hard spheres. Lack of a suitable expansion for the binary kernel in the classical case makes the application of the binary kernel method to classical systems very cumbersome.

Pais and Uhlenbeck have shown in a different way that in the classical limit the binary kernel expansion converges to the Mayer classical expansion. They proceed from the initial assumption that the binary kernel expansion will be identical to the Mayer expansion in the classical limit. This initial assumption permits the derivation of a general formula for the number of Lee-Yang diagrams possible when a given number of binary kernels act. This general formula agrees with the number of diagrams found by direct counting in the classical case. This is proof that the initial assumption of coincidence of the binary kernel expansion with the Mayer expansion in the classical limit is correct.

This work applied the Uhlenbeck and Pais formulation of the binary kernel expansion to the calculation of new quantum mechanical corrections to the third virial coefficient at high temperatures. A form for the binary kernel function which gives the known quantum corrections to the second virial coefficient for hard spheres at high temperatures was found. This form for the binary kernel function failed to give the known first-order quantum correction term for the third virial coefficient. Thus this study gives a form for the binary

kernel function sufficient but not necessary to yield quantum mechanical corrections for hard spheres at high temperatures when used in the binary kernel expansion.

Acknowledgements

I wish to express my sincere gratitude to my Thesis Adviser, Professor Charles E. Hecht of Hunter College for the help and encouragement he gave me especially at crucial stages of the completion of this work.

I also want to thank my wife, Joan, for her understanding and help while I was completing this work.

TABLE OF CONTENTS

LIST OF TABLES

LIST OF FIGURES

INTRODUCTION

The binary kernel method of Lee and Yang[1] is a method of treating the many-body problem in quantum statistical mechanics. In this method diagrams are used to express the effects of interactions among the many particles of a system in terms of a function called the binary kernel function. This binary kernel function can be found from knowledge of how two particles of the system interact. The binary kernel expansion is an expansion of the interaction effects of a many-particle system in terms of the binary kernel function.

The Lee-Yang binary kernel method was developed to treat systems in which quantum mechanical effects are important. It was applied to the calculation of the ground state energy of the Bose-Einstein gas.[2] In the binary kernel method certain cluster functions U_ℓ for a system of ℓ particles are expressed as sums of integrals over powers of the binary kernel starting with the $(\ell - 1)^{st}$ power and continuing to infinite powers in the binary kernel. In treating the Bose-Einstein gas Lee and Yang found an expansion of the binary kernel function which permitted the consideration of lowest order (containing $(\ell - 1)$ binary kernels) and next-to-lowest order (containing ℓ binary kernels) diagrams only in calculating the ground state energy. The use of this method of expanding the binary kernel is the basis of the progress made by Lee and Yang in applying the binary kernel expansion to quantum mechanical systems.

It is the aim of this work to adapt the Lee-Yang binary kernel method to a system obeying classical mechanics. It was planned to investigate the expansion of the equation of state resulting from this

adaptation with the idea of getting new insights into the convergence properties of the virial series and the gaseous condensation problem for a classical system. In the Lee-Yang technique expansion of the binary kernel was found to lead to rapid convergence at low temperature of the binary kernel expansion in the quantum mechanical case. It is found that the development of the binary kernel technique for a classical system requires an infinite summation over all powers of the binary kernel contributing to the expansion. Attempts to find an expansion of the binary kernel function in the classical case which could be used in a way analogous to the treatment of the Bose-Einstein gas by Lee and Yang were not successful. Lack of such an expansion makes the application of the binary kernel method to classical systems very difficult because of the infinite summation required to get the well known classical results for the equation of state.

Pais and Uhlenbeck[3] have shown that the binary kernel expansion of Lee and Yang converges in the classical limit to the Mayer expansion for classical systems. This was done indirectly by working backwards from the initial assumption that the Lee-Yang result is identical to the Mayer expansion in the classical limit. This initial assumption of coincidence with the Mayer results allowed Pais and Uhlenbeck to obtain a general formula for the number of allowed Lee-Yang diagrams given that a certain number of binary kernels are to be operating. That this formula does indeed agree with the number of diagrams found from direct counting in the classical case is proof that the initial assumption is correct; namely that the Lee-

Yang expansion converges to the classical Mayer expansion in the classical limit.

The present work demonstrates the convergence of the Lee-Yang binary kernel expansion in the classical limit to the Mayer expansion for the three and four particle cases directly by applying the classical analogue of the binary kernel function and directly summing up the contributions of all allowed diagrams to obtain the Mayer classical results.

This work also attempted to apply the Lee-Yang binary kernel method to the problem of obtaining new higher order high temperature quantum mechanical corrections (neglecting statistics) to the third virial coefficient. A form for the binary kernel containing quantum corrections sufficient to give the known quantum mechanical corrections to the second virial coefficient was obtained using the Uhlenbeck and Pais form of the binary kernel expansion. The use of this form for the binary kernel to calculate quantum corrections to the third virial coefficient did not check the known quantum corrections to the third virial coefficient. Thus this study gave a sufficient but not necessary form for the binary kernel embodying high temperature quantum mechanical corrections.

Chapter 1

The Binary Kernel Function and Lee-Yang Diagrams

According to the development of the binary kernel expansion by Lee and Yang[1] we consider a system of N particles enclosed in a volume Ω, in the limit $N \longrightarrow \infty$, $\Omega \rightarrow \infty$ with

$$\rho = (N/\Omega)$$

held fixed, being the number density. The Hamiltonian of the system is

$$H = -(\hbar^2/2m) \sum_{i=1}^{N} \nabla_i^2 + \sum_{\substack{ij, \\ i<j}} V_{ij} \tag{1}$$

where

$$V_{ij} = V(\vec{r}_i - \vec{r}_j) \tag{2}$$

is the potential energy between a pair of particles i and j. The mass of a particle is m and $\hbar$ is Planck's constant divided by 2π. The operator W_N is defined by Lee and Yang as

$$W_N = e^{-\beta H_N} \tag{3}$$

where

$$\beta = (1/kT) \tag{4}$$

The matrix element of W_N in coordinate representation is

$$\langle 1',2', \ldots, N' | W_N | 1,2, \ldots, N \rangle =$$

$$\sum_i \psi_i(1',2', \ldots, N') \psi_i^*(1,2, \ldots, N) e^{-\beta E_i} \tag{5}$$

Here the notation is defined by

$$1 = \vec{r}_1 = (x_1, y_1, z_1) \text{ , etc.}$$

$$1' = \vec{r}_1' = (x_1', y_1', z_1') \text{ , etc.} \tag{6}$$

and $\Psi_i(\vec{r}_\nu)$ and E_i are the normalized eigenfunctions and eigenvalues of H_N with periodic boundary conditions in a cubic box of volume Ω. The $\Psi_i(\vec{r}_\nu)$ must be properly symmetrized according to whether the particles obey Fermi-Dirac, Boltzmann, or Bose-Einstein statistics. Following Lee and Yang, the partition function is

$$Q_N = \sum_i e^{-\beta E_i} \tag{7}$$

$$Q_N = \int_\Omega \langle 1,2, \ldots, N | W_N | 1,2, \ldots, N \rangle \, d^{3N}\vec{r} \tag{8}$$

In the development of Lee and Yang the logarithm of the grand partition function is obtained by following a procedure first introduced by Ursell[4] and Mayer[5] for classical statistical mechanics and by Kahn and Uhlenbeck[6] for quantum statistical mechanics; U_ℓ functions are defined by

$$\langle 1' | W_1 | 1 \rangle = \langle 1' | U_1 | 1 \rangle ,$$

$$\langle 1',2' | W_2 | 1,2 \rangle = \langle 1' | U_1 | 1 \rangle \langle 2' | U_1 | 2 \rangle + \langle 1',2' | U_2 | 1,2 \rangle ,$$

$$\begin{aligned} \langle 1',2',3' | W_3 | 1,2,3 \rangle = {} & \langle 1' | U_1 | 1 \rangle \langle 2' | U_1 | 2 \rangle \langle 3' | U_1 | 3 \rangle + \\ & \langle 1' | U_1 | 1 \rangle \langle 2',3' | U_2 | 2,3 \rangle + \\ & \langle 2' | U_1 | 2 \rangle \langle 1',3' | U_2 | 1,3 \rangle + \\ & \langle 3' | U_1 | 3 \rangle \langle 1',2' | U_2 | 1,2 \rangle + \\ & \langle 1',2',3' | U_3 | 1,2,3 \rangle , \ldots \end{aligned} \tag{9}$$

These equations may be inverted to give the U_ℓ as functions of the W_ℓ. Putting $\bar{r}_1 = \bar{r}_1'$, $\bar{r}_2 = \bar{r}_2'$, $\bar{r}_\ell = \bar{r}_\ell'$ in these equations Lee and Yang show that for the grand partition function $\mathcal{Q}$ we may write

$$\mathcal{Q} = \sum_{N=0}^{\infty} (1/N!)\, Q_N z^N \tag{10}$$

$$= \exp\left\{ \sum_{\ell=1}^{\infty} z^\ell (\ell!)^{-1} \int_\Omega \langle 1, \ldots, \ell \mid U_\ell \mid 1, \ldots, \ell \rangle d^{3\ell}\bar{r} \right\} \tag{11}$$

Further, Lee and Yang show that the equilibrium pressure P and density ρ are given by

$$(P/kT) = \lim_{\Omega \to \infty} (\Omega)^{-1} \ln \mathcal{Q} \tag{12}$$

$$\rho = \lim_{\Omega \to \infty} (\Omega)^{-1} \left(\partial \ln \mathcal{Q} / \partial \ln z \right) \tag{13}$$

where the fugacity is defined by

$$z = e^{\beta \mu} \tag{13a}$$

and μ is the chemical potential.

The following relationships are given by Lee and Yang

$$(P/kT) = \lim_{\Omega \to \infty} \sum_{\ell=1}^{\infty} b_\ell z^\ell \tag{14}$$

$$\rho = \lim_{\Omega \to \infty} \sum_{\ell=1}^{\infty} \ell b_\ell z^\ell \tag{15}$$

where the fugacity coefficients b_ℓ are defined by

$$b_\ell = (1/\ell!\Omega) \int \langle 1, \ldots, \ell \mid U_\ell \mid 1, \ldots, \ell \rangle d^{3\ell}\bar{r} \tag{16}$$

In the binary kernel method the functions U_ℓ can be expressed in terms of a function called the binary kernel $B(\beta\,;\,i,j)$ which can be calculated from a solution of the two-body problem.

In the Lee-Yang development the W_N and U_N are treated as operators so that

$$W_N(\beta) = e^{-\beta H_N} \tag{17}$$

where the dependence of W_N on β is emphasized. Writing

$$H_N = T_N + V_N \tag{18}$$

where T_N and V_N are, respectively, the operators for the kinetic and potential energies, we have

$$W_N^0(\beta) = e^{-\beta T_N} = \prod_{i=1} w(\beta\,;\,i) \tag{19}$$

where

$$w(\beta\,;\,i) = e^{(\hbar^2/2m)\beta\,\nabla_i^2} \tag{20}$$

According to Lee and Yang $W_N^0(\beta)$ is a product of N operators each of which operates on the coordinates of one particle. If V is finite, the W_N operators may be expanded into an exponential series in powers of V:

$$W_N(\beta) = W_N^0(\beta) + \int_0^\beta W_N^0(\beta-\beta')(-V_N)W_N^0(\beta')\,d\beta' + \int_0^\beta d\beta' \int_0^{\beta'} d\beta''\, W_N^0(\beta-\beta')(-V_N)W_N^0(\beta'-\beta'') \times (-V_N)W_N^0(\beta'') + \cdots \tag{21}$$

If $V = \infty$ for some configurations, this series ceases to be meaningful. At this point in their development Lee and Yang regard V as finite everywhere and the possibility of V going to infinity is allowed for later in the development.

Lee and Yang represent the sum on the right of equation (21) by diagrams. Each operator contributing to the sum $W_N(\beta)$ is represented by a diagram. Each of the N particles in the system is represented by a vertical line of length β in the diagram for an operator. The vertical lines originate from the same horizontal base level. A horizontal line linking particles i and j stands for an interaction between these particles. No two interactions may occur at the same height in β space above the horizontal base level. Figure 1 gives examples of representing operators by Lee-Yang diagrams. The exact height of a horizontal link in β space is not specified in a diagram because the β primes are to be integrated over, but the order in which the links occur vertically is important. This means that the last two diagrams given for $W_3(\beta)$ in Figure 1 are considered as two different diagrams.

As explained by Lee and Yang, to obtain the operator corresponding to a given diagram a line segment of length γ along the vertical line i i' stands for the operator

$$w(\gamma;i) = e^{(\hbar^2/2m)\gamma\nabla_i^2}$$

A horizontal link between ii' and jj' represents the operator

$$-V(\bar{r}_i - \bar{r}_j)d\beta' = -V_{ij}d\beta'$$

where β' is the height of the link above the base line. The product

of all operators represented by vertical line segments and the horizontal links, integrated over the heights β' of the various links, is the operator represented by a diagram. Further, in the Lee and Yang work, when writing down the operator for a given diagram those operators represented by line segments lower down in the diagram must occur to the right of those represented by line segments higher up in the diagram. Also, the limits of integration of the heights β', β'', ... of the horizontal links are defined by the condition

$$\beta \geq \beta' \geq \beta'' \geq \beta''' \ldots \geq 0 \tag{22}$$

and the relative height of any two links remain of the same sign within the limits of integration as in the diagram.

These rules are clarified by examples given in their work. The diagram for a single particle given in Figure 1 represents the operator

$$W_1(\beta) = w(\beta; 1) = e^{(\hbar^2/2m)\beta\nabla_1^2} \tag{23}$$

The operator corresponding to the diagrams of $W_2(\beta)$ appearing in Figure 1 is given by

$$\begin{aligned} W_2(\beta) = {} & w(\beta; 1)w(\beta; 2) + \int_0^\beta d\beta' w(\beta - \beta'; 1) \\ & \times w(\beta - \beta'; 2)(-V_{12})w(\beta'; 1)w(\beta'; 2) + \\ & \int_0^\beta d\beta' \int_0^{\beta'} d\beta'' w(\beta - \beta'; 1)w(\beta - \beta'; 2)(-V_{12}) \\ & \times w(\beta' - \beta''; 1)w(\beta' - \beta''; 2)(-V_{12})w(\beta''; 1) \\ & \times w(\beta''; 2) \end{aligned} \tag{24}$$

where the three diagrams of $W_2(\beta)$ in Figure 1 correspond to the three terms in equation (24).

Following the development of Lee and Yang, the operator $W_N(\beta)$ is now seen to be the sum of all diagrams of N vertical lines containing all possible interactions consistent with the parameter β. Lee and Yang define a connected diagram as one in which all vertical lines are connected to one another through horizontal links and vertical lines. The nature of the U_2 and U_3 functions as expressed in equations (9) above means that U_2 is the sum of all different connected diagrams for two vertical lines (particles); and that U_3 is the sum of all different connected diagrams for three particles. According to Lee and Yang $U_N(\beta)$ is the sum of all different connected diagrams consisting of N vertical lines and consistent with the parameter β.

The binary kernel $B(\beta; i,j)$ is defined by Lee and Yang as follows:

$$B(\beta; i,j) = (-V_{ij})W_2(\beta) = -V_{ij}e^{-\beta H_2} \tag{25}$$

An explicit operator equation for $U_2(\beta)$ is given by Lee and Yang:

$$U_2(\beta) = e^{-\beta H_2} - e^{(\hbar^2/2m)\beta\nabla_i^2}\, e^{(\hbar^2/2m)\beta\nabla_j^2} \tag{26}$$

equation (26) is then differentiated with respect to β to give a relationship between $B(\beta; i,j)$ and $U_2(\beta)$:

$$B(\beta; i,j) = (\partial U_2(\beta)/\partial\beta) - (\hbar^2/2m)(\nabla_i^2 + \nabla_j^2)U_2(\beta) \tag{27}$$

The procedure followed by Lee and Yang in their work is to first calculate $e^{-\beta H_2}$ using the solutions of the two-body problem for the particle in a box. Then $U_2(\beta)$ is calculated using the operator equation (26) given above. Next equation (27) is used to calculate the binary kernel $B(\beta;i,j)$. The potential energy of interaction V_{ij} does not occur explicitly in these equations so that the binary kernel can be calculated for systems where $V_{ij} = \infty$.

As explained by Lee and Yang, in the binary kernel technique the diagrams of $W_2(\beta)$ can be used with equation (25) defining the binary kernel to adapt a diagramatic representation of the binary kernel as shown in Figure 2. The topmost link in each diagram of Figure 2 represents an additional factor $(-V_{12})$ which has been added. The part of a diagram having this form of repeated links between particles i and j can now be summed up and replaced by a factor $B(\beta; i,j)$. Thus Lee and Yang represent U_ℓ in terms of the binary kernel and give examples for U_2 and U_3 as shown in Figure 3. The algebraic forms of the operators $U_2(\beta)$ and $U_3(\beta)$ can be written down with the aid of the diagrams in Figure 3 as follows:

$$U_2(\beta) = \int_0^\beta d\beta' w(\beta - \beta'; 1) w(\beta - \beta'; 2) B(\beta'; 1,2)$$

$$\begin{aligned} U_3(\beta) = {} & \int_0^\beta d\beta' \int_0^{\beta'} d\beta'' w(\beta - \beta''; 1) w(\beta - \beta'; 2) w(\beta - \beta'; 3) \\ & \times B(\beta' - \beta''; 2,3) B(\beta''; 1,2) w(\beta''; 3) + \\ & \int_0^\beta d\beta' \int_0^{\beta'} d\beta'' w(\beta - \beta'; 1) w(\beta - \beta'; 2) w(\beta - \beta''; 3) \\ & \times B(\beta' - \beta''; 1,2) B(\beta''; 2,3) w(\beta''; 1) + \\ & 4 \text{ other terms of order } \beta^2 + \text{terms of higher order in B} \end{aligned} \qquad (28)$$

The binary kernel technique expresses the cluster functions U_ℓ as sums of integrals over powers of the binary kernel. The fugacity coefficients b_ℓ are integrations of the U_ℓ functions carried out on the coordinates of the particles over the volume open to the particles. The equation of state is expressed in terms of the b_ℓ by the two parametric equations

$$(P/kT) = \sum_{\ell=1}^{\infty} b_\ell \, z^\ell$$

$$\rho = \sum_{\ell=1}^{\infty} \ell b_\ell z^\ell$$

where z is the fugacity,

$$z = e^{\rho\mu}$$

and μ is the chemical potential.

Chapter II

Calculation by Lee and Yang of the Ground State Energy for the Maxwell Boltzmann Gas with Hard Sphere Interaction

Lee and Yang have applied the binary kernel expansion method to the calculation of the ground state energy of a hard sphere Bose-Einstein gas.[2] The Bose-Einstein condensation makes it difficult to approach the limit $T \longrightarrow 0$ for a Bose system. Lee and Yang circumvented this difficulty by making the calculation on the Maxwell-Boltzmann system with hard sphere interaction and noting that at $T = 0$ the thermodynamic properties of a Boltzmann gas are the same as that of the Bose gas.[2]

In the quantum mechanical case the binary kernel B may be expanded in powers of the hard sphere diameter σ:

$$B = B_1 + B_2 + \ldots \tag{1}$$

where B_1 is of order σ, B_2 is of order σ^2, etc..[2] The fugacity coefficients b_ℓ are integrals over the Ursell cluster functions U_ℓ. The U_ℓ functions are expressed in the binary kernel method as sums of integrals over powers of the binary kernel B, starting with the $(\ell - 1)^{st}$ power. The diagrams of U_ℓ which contain $(\ell - 1)$ binary kernels are called lowest order diagrams and those which contain ℓ binary kernels are called next-to-lowest order diagrams.[2] For each ℓ, Lee and Yang calculate the dominant terms in b_ℓ. They take as the dominant terms in b_ℓ those represented by the lowest

order and next-to-lowest order diagrams. These dominant terms have the following form[2]:

$$b_\ell = \lambda^{-3}\left[\gamma_\ell\,(\sigma/\lambda)^{\ell-1} + \delta_\ell\,(\sigma/\lambda)^{\ell} + \ldots\right] \tag{2}$$

where λ is the de Broglie thermal wavelength

$$\lambda = h(\beta/2\pi m)^{1/2}$$

The coefficients γ_ℓ and δ_ℓ are pure numbers. The generating functions $\Gamma(x)$ and $\Delta(x)$ are defined as follows.[2]

$$\Gamma(x) = \sum_{\ell=1}^{\infty} \gamma_\ell\,(x/2)^{\ell} \tag{3}$$

$$\Delta(x) = \sum_{\ell=1}^{\infty} \delta_\ell\,(x/2)^{\ell} \tag{4}$$

Using the fugacity series for the pressure

$$\beta P = \sum_{\ell=1}^{\infty} b_\ell\, z^{\ell} \tag{5}$$

where z is the fugacity and is related to the chemical potential μ by $z = \exp(\mu/kT)$. The pressure is obtained as a function of the generating functions[2] by

$$P = (h^2/2\pi m)\left[(\sigma\lambda)^{-4}\Gamma(x) + \lambda^{-5}\Delta(x) + \ldots\right] \tag{6}$$

where

$$x = (2\sigma z/\lambda)$$

In the limit $T \longrightarrow 0$, $\lambda \longrightarrow \infty$, so that successive terms in this expansion become increasingly unimportant. In the limit $T \rightarrow 0$ the

generating functions $\Gamma(x)$ and $\Delta(x)$ have the forms[2]

$$\Gamma(x) \longrightarrow (\pi^2 m^2/h^4)\mu^2\lambda^4 \tag{7}$$

$$\Delta(x) \longrightarrow -(128\pi^2 m^{5/2}/15h^5)\mu^{5/2}\lambda^5 \tag{8}$$

so that the following expression for the pressure at T = 0 is obtained[2]

$$(P)_{T=0} = (\pi m/2h^2\sigma)\mu^2 - (64\pi m^{3/2}/15h^3)\mu^{5/2} + \ldots \tag{9}$$

Using the thermodynamic equation

$$dP = \rho\, d\mu + (S/\mathcal{V})dT \tag{10}$$

The particle density at T = 0 is obtained[2]

$$(\rho)_{T=0} = (\pi m\mu/h^2\sigma) - (32\pi m^{3/2}/3\,h^3)\mu^{3/2} + \ldots \tag{11}$$

The energy density at T = 0 is given by[2]

$$(E/\mathcal{V})_{T=0} = \left[\mu(d/d\mu) - 1\right](P)_{T=0} \tag{12}$$

$$(E/\mathcal{V})_{T=0} = (\pi m\mu^2/2\,h^2\sigma) - (32\pi m^{3/2}\mu^{5/2}/5\,h^3) \tag{13}$$

Eliminating μ gives the ground state energy per particle[2]

$$(E/N)_{T=0} = (2\pi\hbar^2\rho\sigma/m)\left[1 + (128/15)(\sigma^3\rho/\pi)^{1/2}\right] \tag{14}$$

In this calculation for a quantum mechanical system an appropriate expansion of the binary kernel has been used. In doing the sum of the b_ℓ over all ℓ the contributions from the $(\ell - 1)^{st}$

and ℓ^{th} powers of the binary kernel are retained for each ℓ. This development was studied with a view to dealing with the parametric equations of state

$$\beta P = \sum_{\ell=1}^{\infty} b_\ell z^\ell$$

$$\rho = \sum_{\ell=1}^{\infty} \ell b_\ell z^\ell$$

for a classical system of hard spheres in an analogous manner. It was planned to develop an appropriate expansion of the binary kernel function for the classical system with hard sphere interaction. The contributions of the $(\ell - 1)^{st}$ and ℓ^{th} powers of the binary kernel could be retained in doing the sums over ℓ to eliminate the fugacity z between the two equations in order to obtain the series for the pressure in powers of the density (virial series) for the hard sphere gas. Such a program could not be carried out because a useful expansion of the binary kernel function for the classical system could not be developed.

Chapter III

An Alternative Derivation of the Numbers of Lowest Order and Next-to-Lowest Order Lee-Yang Diagrams

In the binary kernel technique as used by Lee and Yang, for each ℓ the dominant terms in b_ℓ are calculated. The dominant terms are taken by Lee and Yang as those represented by the lowest order and next-to-lowest order diagrams.[2]

As discussed by Lee and Yang,[2] there is a one-to-one correspondence between the lowest order diagrams for b_ℓ and "tree skeletons". This is shown in Figure 4. The tree skeletons are defined by Lee and Yang as connected diagrams of ℓ particles, connected by $(\ell - 1)$ links. Lee and Yang did not calculate explicitly the number of lowest order diagrams for each ℓ but summed up their contributions to b_ℓ using a method involving generating functions. The number of these tree skeletons (lowest order diagrams) for each ℓ is given by the formula

$$\ell^{\ell-2}\,[(\ell - 1)]\,! \tag{1}$$

This is true because there are $\ell^{\ell-2}$ ways[7] of making connected diagrams having ℓ points with $(\ell - 1)$ lines (binary kernels) linking them. The factor $(\ell - 1)!$ comes about because the $(\ell - 1)$ distinct links in any diagram may be arranged in $(\ell - 1)!$ ways in ξ sequence. The ξ sequence determines the order in which the binary kernels operating between the particles act. It is im-

possible for the binary kernel operator to act between the same two particles in immediate succession in β sequence.

Each next-to-lowest order Lee-Yang diagram contains ℓ binary kernels. The next-to-lowest order diagrams are diagrams of ℓ points with ℓ links or lines joining the points. Lee and Yang draw skeltons to represent these next-to-lowest order diagrams as shown in Figure 5.[2] Each such skeleton consists of ℓ numbered points connected by ℓ lines, μ of which form a simple loop, the rest not forming loops. The case $\mu = 2$ is special because the loop is not a polygon but a repetition of the single line between two particles. In the Lee-Yang method of counting each line is given a β label which determines the order in which the binary kernel operators act in the diagram. The one line which is doubled receives two β labels, β_m and β_n. Because the binary kernel operator cannot operate between the same two particles twice in succession $|m - n| \neq 1$.[2] Lee and Yang enumerate the diagrams by first drawing all unlabelled skeletons and then generating all possible diagrams by considering all possible labellings with β . Each of the resulting labelled skeletons corresponds uniquely to a single next-to-lowest order diagram. In their treatment of the next-to-lowest order diagrams Lee and Yang have not calculated explicitly the numbers of diagrams but have summed up their contributions to b_ℓ using generating function methods.

The number of diagrams containing ℓ points with ℓ lines joining them and no line repeated ($\mu \neq 2$) has been obtained in graph theoretical calculations. These diagrams consist of polygons with $(\ell - \delta)$ sides and δ lines hung on the vertices. Their number $C_{\ell,\ell}$ is

given by[8]

$$C_{\ell,\ell} = \sum_{\delta=0}^{\delta=\ell-3} (\ell^{\delta}/\delta!)\left[(\ell-1)!/2\right] \qquad (2)$$

where δ is the number of free lines in the diagram. The free lines are those lines not forming the polygon. Each addend in equation (2) corresponds to a different polygon with free lines hung on its vertices. Thus when $\delta = 0$ we have the ℓ-sided polygon with no free lines. The value $\delta = 1$ corresponds to the $\ell - 1$ sided polygon with one free line to be hung on its vertices, etc. To get the total number of next-to-lowest order diagrams with $\mu \geq 3$ we multiply equation (2) by $\ell!$ to take into account the different possible arrangements in β sequence of the ℓ distinct binary kernels involved in the diagram. When $\mu = 2$ multiplication by $\ell!$ is not correct because two of the links operate between the same two particles and cannot be adjacent to one another in β sequence.

The diagrams of ℓ points and ℓ lines with $\mu = 2$ have two links occurring between the same two particles and $\ell - 2$ distinct links linking different particles. As pointed out by Lee and Yang the repeated link in these diagrams cannot be labelled by two consecutive β labels. As can be seen in Figure 5 switching the order in which the repeated binary kernels act does not lead to a new skeleton. Thus for the case $\mu = 2$ the total number of skeletons obtained by considering different labellings must be divided by two. This necessity of division

by two is also shown by the result of using the addend of equation (2) corresponding to $\mu = 2$ to give the number of such unlabelled skeletons:

$$\frac{\ell^{\ell-2}(\ell-1)}{2} \tag{3}$$

This result may be obtained also by considering that the number of unlabelled skeletons of ℓ points containing $(\ell-1)$ binary kernels is given by $\ell^{\ell-2}$. Since there are $\ell-1$ links and we are to repeat one link, we have $\ell-1$ choices for the repeated link so that the number of these unlabelled skeletons is given by

$$\ell^{\ell-2}(\ell-1)$$

and division by two will be necessary in labelling with β's. Equation (3) is consistent with the result given by Lee and Yang.[2]

We cannot simply multiply equation (3) above by $\ell!$ to count the number of arrangements in β sequence for these diagrams. This is because of the restriction on arrangements of the links in β sequence for the case $\mu = 2$ discussed earlier. We must multiply by $\ell! f$ where f is a factor smaller than unity and is given by

$$f = \frac{(\ell-2)}{\ell} \tag{4}$$

That f should have the form given by equation (4) is shown by the following. There are ℓ available positions in β space for the ℓ links in each of the next-to-lowest order diagrams with

$\mu = 2$. Suppose we place one of the repeated links in the lowest (first) position in β sequence. Since the other repeated link cannot occupy the position immediately adjacent to the first position, there are $\ell - 2$ positions where it may be located. In each of these $\ell - 2$ arrangements of the repeated links the other $\ell - 2$ different links can be arranged in $(\ell - 2)!$ ways. Thus there are $(\ell - 2)\,[\ell - 2]!$ arrangements in β sequence in which the lowest β position is occupied by one of the repeated links.

If one of the repeated links is placed in the second or next to the bottom β position, these are $(\ell - 3)$ positions in which the other repeated link may be placed. (The bottom and the third β position are not allowed.) Again for each of these $(\ell - 3)$ arrangements of the repeated links the other $(\ell - 2)$ different links may be arranged in $(\ell - 2)!$ ways. This counts all arrangements in β space in which the second position in β space is occupied by one of the repeated links.

If we decide to place one of the repeated links in the third β position, there are $\ell - 4$ positions open to the other repeated link. (Although position one is not adjacent to position three and thus is available we have already counted all arrangements in which one of the repeated links is found in position one.) Again the other $\ell - 2$ different links can be arranged in $(\ell - 2)!$ ways in each of the $\ell - 4$ arrangements of the repeated links.

Continuation of this process shows that in general the number of arrangements in β sequence for the ℓ links two of

which link the same two particles is given by

$$[(\ell - 2) + (\ell - 3) + \ldots + 1](\ell - 2)!$$

$$= (\ell - 2)! \sum_{n=1}^{\ell-2} n = \frac{(\ell - 1)(\ell - 2)}{2} (\ell - 2)! \tag{5}$$

Then the total number of diagrams of ℓ points with ℓ links in which one link is repeated ($\mu = 2$) is given by

$$\ell^{\ell-2} (\ell - 1) \frac{(\ell - 1)(\ell - 2)}{2} (\ell - 2)!$$

$$= \frac{\ell^{\ell-2} (\ell - 1)}{2} \ell! [(\ell - 2)/\ell] \tag{6}$$

As noted above this is consistent with Lee and Yang's division by two to correct for the repeated link. We find here that multiplication by

$$\ell! \frac{\ell - 2}{\ell} \tag{7}$$

gives the correct count for these next-to-lowest order diagrams with $\mu = 2$. The factor f mentioned above is then given by

$$f = \frac{\ell - 2}{\ell} \tag{8}$$

We have found that the number of next-to-lowest order diagrams is given by

$$C_{\ell,\ell} \ell! + \ell^{\ell-2} \frac{(\ell - 1)}{2} \ell! \frac{\ell - 2}{\ell} \tag{9}$$

Chapter IV

Application of the Binary Kernel Method to a Classical Gas with Hard-Sphere Interaction

The binary kernel technique of Lee and Yang is now adapted to a classical gas of hard spheres. It is used to calculate the fugacity coefficients (Mayer cluster integrals) b_3 and b_4 from which the third and fourth virial coefficients for hard spheres may be obtained. It is found that the fugacity coefficients b_ℓ so obtained lead to the known virial coefficients only if the number of binary kernels acting is allowed to become infinite, and a summation is carried out over all resulting diagrams which then contribute. Summing over all diagrams arising when only some finite number of binary kernels act is unsatisfactory.[9]

The form of the Ursell cluster function $U_2(\beta)$ is given by Lee and Yang for a quantum mechanical system as the operator $U_2(\beta)$[1]

$$U_2(\beta) = e^{-\beta H_2} - e^{+\beta(\hbar^2/2m)\nabla_1^2} e^{+\beta(\hbar^2/2m)\nabla_2^2} \tag{1}$$

where

$$H_2 = -\sum_{i=1}^{2} (\hbar^2/2m)\nabla_i^2 + V(\bar{r}_1 - \bar{r}_2)$$

$V(\bar{r}_1 - \bar{r}_2)$ = potential of interaction for molecules 1 and 2

$\hbar = (h/2\pi)$

In the classical application this form is replaced by its classical analogue,

$$U_2(\beta) = (1/h^6) \int_{\bar{p}_1} \int_{\bar{p}_2} \left[e^{-\beta H_2} - e^{-\beta(\bar{p}_1^2/2m)} \, e^{-\beta(\bar{p}_2^2/2m)} \right] d\bar{p}_1 d\bar{p}_2$$

$$H_2 = \sum_{i=1}^{2} (\bar{p}_i^2/2m) + V(\bar{r}_1 - \bar{r}_2) \tag{2}$$

Introducing the relative coordinate r_{12},

$$r_{12} = |\bar{r}_1 - \bar{r}_2|$$

$$U_2(\beta) = (1/h^6) \int_{\bar{p}_1} \int_{\bar{p}_2} e^{-\frac{\beta}{2m}(\bar{p}_1^2 + \bar{p}_2^2)} \left[e^{-\beta V(r_{12})} - 1 \right] d\bar{p}_1 d\bar{p}_2 \tag{3}$$

$$U_2(\beta) = \lambda^{-6} \left[e^{-\beta V(r_{12})} - 1 \right] \tag{4}$$

where

$$\lambda = (h^2\beta/2\pi m)^{1/2} \tag{5}$$

as discussed by Lee and Yang[1] $U_2(\beta)$ is required by definition to be zero when $\beta = 0$. The form in equation (4) above does not satisfy this so a step function $\Delta(\beta)$

must be added:

$$U_2(\beta) = (1/h^6)\iint e^{-\frac{\beta}{2m}(\bar{p}_1^{\,2} + \bar{p}_2^{\,2})}\left[e^{-\beta V(r_{12})} - 1\right] d\bar{p}_1 d\bar{p}_2 +$$

$$\Delta(\beta)(1/h^6)\iint e^{-\frac{\beta}{2m}(\bar{p}_1^{\,2} + \bar{p}_2^{\,2})}\left[1 - e^{-\beta V(r_{12})}\right] d\bar{p}_1 d\bar{p}_2 \qquad (6)$$

where

$$\Delta(\beta) = 1 \quad \text{for } \beta \leq 0$$

$$\Delta(\beta) = 0 \quad \text{for } \beta > 0 \qquad (7)$$

The operator $U_2(\beta)$ is related to the binary operator in quantum mechanics as follows:[1]

$$B(\beta;\ 1,2) = \frac{\partial}{\partial\beta} U_2(\beta) + (\hbar^2/2m)(\nabla_1^{\,2} + \nabla_2^{\,2})U_2(\beta) \qquad (8)$$

This gives for $B(\beta;1,2)$ for a system obeying classical mechanics:

$$B(\beta;\ i,j) = (1/h^6)\int_{\bar{p}_1}\int_{\bar{p}_2} e^{-(\beta/2m)(\bar{p}_i^{\,2} + \bar{p}_j^{\,2})}\left[\frac{\partial}{\partial\beta} f_{ij}(\beta) +\right.$$

$$\left. -\Delta(\beta)\frac{\partial}{\partial\beta} f_{ij}(\beta) + f_{ij}(\beta)\,\delta(\beta)\right] d\bar{p}_i d\bar{p}_j \qquad (9)$$

where the Mayer function $f_{ij}(\beta)$ is defined by

$$f_{ij}(\beta) = (e^{-\beta V(r_{ij})} - 1)$$

In all applications of the binary kernel we shall leave the integrations over momenta (which are trival in the classical case) until last and apply $B(\beta;i,j)$ in the form

$$B(\beta;\, i,j) = e^{-(\beta/2m)(\bar{p}_i^{\,2} + \bar{p}_j^{\,2})} \left[\frac{\partial}{\partial \beta} f_{ij}(\beta) + \right.$$

$$\left. - \Delta(\beta) \frac{\partial}{\partial \beta} f_{ij}(\beta) + f_{ij}(\beta)\, \delta(\beta) \right] \tag{10}$$

it being understood that integrations over the momenta will be performed as the last step.

For a hard-sphere potential of diameter σ,

$$V(r_{ij}) = \infty \,, \quad 0 < r_{ij} < \sigma$$

$$V(r_{ij}) = 0 \,, \quad r_{ij} > \sigma \tag{11}$$

the binary kernel becomes

$$B(\beta;\, i,j) = e^{-(\beta/2m)(\bar{p}_i^{\,2} + \bar{p}_j^{\,2})} f_{ij}(\beta)\, \delta(\beta) \tag{12}$$

because

$$\frac{\partial}{\partial \beta} f_{ij}(\beta) = 0 \tag{13}$$

for the hard-sphere interaction.

The ℓ^{th} fugacity coefficient b_ℓ is given by Lee and Yang as

$$b_\ell = (\Omega\, !)^{-1} \int \cdots \int U_\ell \, d\bar{r}_1 \cdots d\bar{r}_\ell \tag{14}$$

where

$$\Omega = \text{volume open to the } \ell \text{ particles} \tag{14a}$$

as we have seen, the U_ℓ are related to the binary kernel through the use of diagrams. For U_2 we have

$$U_2(\beta) = \int_0^\beta d\beta' w(\beta - \beta' ;1) w(\beta - \beta';2) B(\beta' ;1,2) \tag{15}$$

The $w(\beta;i)$ functions are defined by Lee and Yang as[1]

$$w(\beta ;i) = e^{\beta (\hbar^2/2m) \nabla_i^2} \tag{16}$$

and have the classical form

$$w(\beta ;i) = e^{-\beta (\bar{p}_i^{\,2}/2m)} \tag{17}$$

Using equations (12), (15) and (17) in equation (14) gives for b_2

$$b_2 = (2\pi)^{-1} \iint e^{-(\beta/2m)(\bar{p}_1^{\,2} + \bar{p}_2^{\,2})} \chi \int_0^\beta d\beta' \, f_{12}(\beta') \, \delta(\beta') d\bar{r}_1 d\bar{r}_2 \tag{18}$$

To obtain b_ℓ from U_ℓ we integrate over the coordinates first. This followed by the integration over β' which gives a factor unity, and the momenta integrations gives

$$b_2 = -\lambda^{-6} b_o \tag{19}$$

with

$$b_o = (2\pi\sigma^3/3)$$

This leads to the known result for the second virial coefficient B_2 for hard spheres since $b_1 = \lambda^{-3}$ and

$$B_2 = -Nb_2(b_1)^{-2} \tag{20}$$

For the square-well interaction

$$\begin{aligned} V(r_{ij}) &= \infty \qquad 0 < r_{ij} < \sigma \\ V(r_{ij}) &= -\varepsilon \qquad 0 < r_{ij} < g\sigma \\ V(r_{ij}) &= 0 \qquad\quad r_{ij} > g\sigma \end{aligned} \tag{21}$$

the binary kernel is

$$B(\beta; i,j) = e^{-(\beta/2m)(\bar{p}_i^2 + \bar{p}_j^2)} \left[\frac{\partial}{\partial\beta} f_{ij}(\beta) + f_{ij}(\beta)\,\delta(\beta) \right] \tag{22}$$

Using this in equations (14), (15) and integrating over coordinates first, followed by the β integration and doing the momenta integrals as the final step gives b_2 for the square-well interac-

tion

$$b_2 = -\lambda^{-6} b_o \left[1 - (e^{+\beta\varepsilon} - 1)(g^3 - 1)\right] \tag{23}$$

which gives the well-known form for the second virial coefficient for the square-well interaction.

To calculate b_3 for hard spheres we must consider the diagrams of U_3. The six lowest order diagrams for U_3 are shown in Figurgrams of U_3. The six lowest order diagrams for U_3 are shown in adding an additional binary kernel to each of the lowest order diagrams. Because two binary kernels cannot operate between the same two particles in succession, the topmost link in each of the six diagrams cannot be repeated as the added binary kernel. Therefore, in the U_3 case for each lowest order diagram, there are only two choices for the added binary kernel, since among the three particles there is a total of three links. This means we can add the third link to each of the lowest order diagrams in two ways giving 12 next-to-lowest order diagrams. The same considerations give 24 diagrams of U_3 containing 4 kernels, 48 diagrams containing 5 kernels, etc.

The six lowest order diagrams of U_3 are all of the same topological type meaning they give the same integral over coordinates. A typical one of these has the form[1]

$$U_3' = \int_0^\beta d\beta' \; d\beta'' w(\beta - \beta''; 1) w(\beta - \beta'; 2) \times w(\beta - \beta'; 3) B(\beta' - \beta''; 2,3) B(\beta''; 1,2) w(\beta''; 3) \tag{24}$$

(In this notation U_3' indicates a single specific diagram of U_3, and b_3' indicates the integral contribution of such a diagram to b_3.) Using equation (12) for the binary kernel, we have

$$U_3' = e^{-(\beta/2m)(\bar{p}_1^2 + \bar{p}_2^2 + \bar{p}_3^2)} \int_0^{\beta} d\beta' \int_0^{\beta'} d\beta'' f_{23}(\beta' - \beta'')$$

$$\times f(\beta' - \beta'') f_{12}(\beta'') \delta(\beta'') \tag{25}$$

The Mayer functions satisfy the following

$$f_{ij}(\beta) = -1 \qquad 0 < r_{ij} < \sigma$$

$$f_{ij}(\beta) = 0 \qquad r_{ij} > \sigma \tag{26}$$

The integration over coordinates in equation (25), including the factor $(\Omega)^{-1}$ as in equation (14), followed by integration over β' and β'' and the momenta integrations, results in a contribution to $3!b_3$ of

$$3!b_3' = \lambda^{-9}(4b_o^2) \tag{27}$$

The next-to-lowest order diagrams consist of two topological types as shown in Figure 7. The type I_2 diagram has the form

$$U_3' = e^{-(\beta/2m)(\bar{p}_1^2 + \bar{p}_2^2 + \bar{p}_3^2)} \int_0^{\beta} d\beta' \int_0^{\beta'} d\beta'' \int_0^{\beta''} d\beta''' \times$$

$$\times f_{12}(\beta' - \beta'')\delta(\beta' - \beta'')f_{23}(\beta'' - \beta''')$$

$$\times\delta(\beta'' - \beta''')f_{12}(\beta''')\delta(\beta''') \tag{28}$$

Because of the nature of the Mayer functions, the diagrams of topological type I_2 give the same numerical contribution to b_3 as the diagram of equation (24), but the additional binary kernel changes the sign of this contribution. The diagram of type I_3 has the form

$$U_3' = e^{-(\beta/2m)(\bar{p}_1^2 + \bar{p}_2^2 + \bar{p}_3^2)} \int_0^{\beta} d\beta' \int_0^{\beta'} d\beta'' \int_0^{\beta''} d\beta'''$$

$$\times f_{13}(\beta' - \beta'')\delta(\beta' - \beta'')f_{23}(\beta'' - \beta''')$$

$$\delta(\beta'' - \beta''')f_{12}(\beta''')\delta(\beta''') \tag{29}$$

and gives a contribution to $3!b_3$ of

$$3!b_3' = -\lambda^{-9}(15b_o^2/8) \tag{30}$$

Addition of another binary kernel to this diagram gives a fourth-order diagram with identical numerical contribution but differing in sign.

The U_3 diagrams consist of the two topological types I_2 and I_3. The absolute values of the integral contributions of these are $\lambda^{-9}(4b_o^2)$ and $\lambda^{-9}(15b_o^2/8)$; respectively. The sign of the contribution of a diagram is given by the factor $(-1)^n$, where n is the number of binary kernels in the diagram.

We find that b_3 can be expressed as

$$3!\, b_3 = 6\, I_2 - (6\, I_2 + 6\, I_3) +$$

$$+ 6\, I_2 + (24 - 6)\, I_3 - \ldots \tag{31}$$

where I_2 and I_3 are given by

$$I_2 = \lambda^{-9}(4b_o^2)$$

$$I_3 = \lambda^{-9}(15b_o^2/8) \tag{32}$$

After some algebra equation (31) becomes

$$3!\, b_3 = (6\, I_2 - 6\, I_3) \sum_{n=0}^{\infty} (-1)^n + 6\, I_3 \sum_{n=0}^{\infty} (-2)^n \tag{33}$$

Using the analytical continuation of

$$\sum_{n=0}^{\infty} (-x)^n \tag{34}$$

along the positive real axis not enclosing the singularity on the negative real axis at $x = -1$,

$$\sum_{n=0}^{\infty} (-x)^n = (1 + x)^{-1} \tag{34a}$$

and

$$b_3 = (1/3!)(3\, I_2 - I_3) = \lambda^{-9}(27b_o^2/16) \tag{35}$$

which leads to the known result for the third virial coefficient for hard spheres.

We recall that there is a one-to-one correspondence between the lowest order diagrams for b_ℓ and "tree skeletons", and that the number of these tree skeletons is given by[7]

$$\ell^{\ell-2}(\ell-1)! \tag{36}$$

The 96 lowest order diagrams for b_4 consist of 72 tree skeletons of type (a) and 24 of type (b) shown in Figure 8. We will generate the higher order diagrams of U_4 which come from these connected lowest order diagrams by adding binary kernels to them. The sign of a contribution of a diagram is obtained as in the b_3 case. In this four particle case, a new link may be added to a diagram in five ways, the topmost link being ruled out as before. The transformation properties of the various diagrams in the four particle case are shown in Figure 8.

We use the transformation properties of the various diagrams to sum up the contributions of the different topological types to b_4. We first sum the contribution of the diagrams of type (a). (The lower case letters in parentheses here refer to the diagrams in Figure 8.) Using the transformation properties for type (a) we have for type (a) diagrams as more binary kernels are added:

3 kernels	4 kernels	5 kernels
$-72(1)$ type (a)	$+72(2)$ type (a)	$-72(2)^2$ type(a)

6 kernels ...

$+72(2)^3$ type (a)

so that the total number of type (a) diagrams contributing after an infinite number of binary kernels are added is given by

$$-72\left[1 + (-2) + (-2)^2 + (-2)^3 + \ldots +\right] \tag{37}$$

$$=-72 \sum_{n=0}^{\infty} (-2)^n = -24 \tag{38}$$

This means -24 type (a) diagrams is the net number of this type coming from the connected lowest order diagrams containing $(\ell - 1)$ binary kernels. The 24 type (b) diagrams transform into themselves in the same way as do the type (a). Therefore, we may sum up the type (b) diagrams in the same manner to give -8 type (b) diagrams coming from connected lowest order diagrams of U_4.

In order to sum the type (c) diagrams we note that they are produced at four binary kernels from type (a) diagrams according to the transformation properties given in Figure 8. We obtain two of the type (c) diagrams from each type (a) diagram, and then these two type (c) diagrams transform to give three type (c) diagrams. We have summed the type (a) diagrams according to equations (37) and (38). Therefore, for type (c) diagrams coming from type (a) diagrams present at three binary kernels in U_4 we have:

4 kernels	5 kernels	6 kernels
$+(2)72(1)$	$-(2)72(2)$ $-(3)(2)72(1)$	$+(2)72(2)^2$ $+(3)(2)72(2)$ $+(3)^2(2)72(1)$

7 kernels ...

$(-2)72(2)^3$
$(-3)(2)72(2)^2$
$-(3)^2(2)72(2)$
$-(3)^3(2)72(1)$

This may be written

$$(2)72\left\{+1 + (-1)\left[2 + 3\right] + \left[(2)^2 + (3)(2) + (3)^2\right] + \right.$$

$$\left. + (-1)\left[(2)^3 + (3)(2)^2 + (3)^2(2) + (3)^3\right] + \ldots \right\} \tag{39}$$

$$= (2)72\left\{\sum_{n=0}^{\infty} (-1)^n \left[x^n + x^{n-1}y + x^{n-2}y^2 + \ldots + x^2y^{n-2} + xy^{n-1} + y^n\right]\right\} \tag{40}$$

where

$$x = 2$$

$$y = 3 \tag{41}$$

Then the sum for type (c) diagrams can be written

$$2(72)\left\{\sum_{n_1=0}^{\infty} (-x)^{n_1} \sum_{n_2=0}^{\infty} (-y)^{n_2}\right\} = 12 \quad \square \tag{42}$$

which is the net number of type (c) diagrams coming from type (a) at three kernels in U_4.

Consideration of the transformation properties of the 24 type (b) diagrams present at three kernels leads to a similar sum for the type (c) diagrams coming from these 24 type (b) diagrams. We have for type (c) coming from these type (b):

$$(3)(24)\Big\{1 + (-1)\,[2+3] + \left[(2)^2 + (2)(3) + (3)^2\right] + \\ + (-1)\left[(2)^3 + (2)^2(3)^2 + (2)(3)^2 + (3)^3\right] + \ldots +\Big\}$$

$$= (3)(24)\left\{\sum_{n_1=0}^{\infty} (-x)^{n_1} \sum_{n_2=0}^{\infty} (-y)^{n_2}\right\} = 6 \square \tag{43}$$

which is the net number of type (c) diagrams coming from the type (b) diagrams present at three kernels in U_4.

To get the number of type (d) diagrams arising from the connected diagrams entering at three kernels in U_4 we see from Figure 8 that each type (a) diagram gives one type (d) diagram and that this type (d) transforms to give three type (d) diagrams. Recalling the sum on type (a) given in equation (38), we have for type (d) diagrams coming from this source:

4 kernels	5 kernels	6 kernels	7 kernels	...
$+72(1)$	$-72(2)$	$+72(2)^2$	$-72(2)^3$	
	$-72(3)$	$+72(2)(3)$	$-72(2)^2(3)$	
		$+72(3)^2$	$-72(2)(3)^2$	
			$-72(3)^3$	

which may be written

$$72 \left\{ \sum_{n=0}^{\infty} (-1)^n \left[x^n + x^{n-1}y + x^{n-2}y^2 + \ldots + x^2y^{n-2} + xy^{n-1} + y^n \right] \right\} \tag{44}$$

$$= 72 \sum_{n_1=0}^{\infty} (-x)^{n_1} \sum_{n_2=0}^{\infty} (-y)^{n_2} = 6 \square \tag{45}$$

where

$$x = 2$$
$$y = 3 \tag{46}$$

Thus equation (45) gives the net number of type (d) diagrams coming from the connected lowest order diagrams present at 3 kernels in U_4.

We now sum the type (e) diagrams coming from the lowest order connected diagrams entering at three kernels. The type (e) diagrams are generated from type (d) according to the transformation property shown in Figure 8. Each type (d) diagram gives two type (e) diagrams which in turn transform to give four type (e) diagrams. Recalling our work leading to equation (45) we wrote the type (d) diagrams as follows:

4 kernels	5 kernels	6 kernels
$72\{1\}$	$72\{(-1)[2+3]\}$	$72\{[(2)^2 + (2)(3) + (3)^2]\}$

$$72\{(-1)[(2)^3 + (2)^2(3) + (2)(3)^2 + (3)^3$$
$$72\{(-1)[(2)^3 + (2)^2(3) + (2)(3)^2 + (3)^3]\}$$

8 kernels ...

$$72\left\{\left[(2)^4 + (2)^3(3) + (2)^2(3)^2 + (2)(3)^3 + (3)^4\right]\right\}$$

Then using the transformation property of type (d) and the transformation property of type (e) we have for the type (e) diagrams:

5 kernels

$$-72\{1\}(2)$$

6 kernels

$$-72\{(-1)[2+3]\}(2)$$
$$+72\{1\}(2)(4)$$

7 kernels

$$-72\left\{\left[(2)^2 + (2)(3) + (3)^2\right]\right\}(2)$$
$$+72\left\{(-1)[2+3]\right\}(2)(4)$$
$$-72\{1\}(2)(4)^2$$

8 kernels

$$-72\left\{(-1)\left[(2)^3 + (2)^2(3) + (2)(3)^2 + (3)^3\right]\right\}(2)$$
$$+72\left\{\left[(2)^2 + (2)(3) + (3)^2\right]\right\}(2)(4)$$
$$-72\left\{(-1)[2+3]\right\}(2)(4)^2$$
$$+72\{1\}(2)(4)^3$$

...

which may be written

$$-72(2)\Big\{1 + \left[(-1)(2+3) + (-4)\right] + \left[(2)^2 + (2)(3) + (3)^2 + (2+3)(4) + (4)^2\right] + \left[(-1)\left[(2)^3 + (2)^2(3) + (2)(3)^2 + (3)^3\right] + \left[(2)^2 + (2)(3) + (3)^2\right](-4) + (-1)[2+3](4)^2 - (4)^3\right] + \ldots\Big\} \tag{47}$$

$$= \sum_{m=0}^{\infty} (-4)^m \left\{ (-2)(72) \sum_{n=0}^{\infty} (-1)^n \left[x^n + x^{n-1}y + \ldots + xy^{n-1} + y^n \right] \right\} 36$$

$$= (12/5) \boxtimes \tag{48}$$

where

$$x = 2$$

$$y = 3 \tag{49}$$

which is the number of type (e) diagrams coming from the type (d) diagrams present at four kernels.

The type (e) diagrams also arise from type (c) diagrams. Each type (c) diagram transforms to give two type (e) diagrams each of which then gives four type (e) diagrams as more kernels are added. We summed the type (c) diagrams in equations (40) to (43). By considerations very similar to our treatment above for type (e) diagrams coming from type (d) diagrams we get the following sum for the type (e) diagrams coming from type (c) diagrams:

$$\sum_{m=0}^{\infty} (-4)^m \left\{ -2 \left[(2)72 \sum_{n=0}^{\infty} (-1)^n \left[x^n + x^{n-1}y + \ldots + xy^{n-1} + y^n \right] + \right.\right.$$

$$\left.\left. + 3(24) \sum_{n=0}^{\infty} (-1)^n \left[x^n + x^{n-1}y + \ldots + xy^{n-1} + y^n \right] \right] \right\} \tag{50}$$

$$= \sum_{m=0}^{\infty} (-4)^m \left\{ (-2) \left[12 + 6 \right] \right\} = (-36/5) \boxtimes \tag{51}$$

which is the number of type (e) diagrams coming from the connected type (c) diagrams entering at 4 kernels.

Combining equations (48) and (51) gives $\frac{-48}{5}$ type (e) diagrams for the net number of type (e) coming from connected lowest

order diagrams in U_4.

Type (f) diagrams come only from the type (e) diagrams. Each type (e) gives one type (f) and each of these type (f) diagrams goes on to give five additional type (f) diagrams as more binary kernels are added. By consideration of the numbers of type (e) diagrams in each order and the transformation properties of these to give the type (f) diagrams but omitting the enumeration of the type (f) diagrams contributing as each new binary kernel is added, we have

$$\sum_{m=0} (-5)^m \left\{(1)(12/5) + (1)(36/5)\right\} = (8/5) \boxtimes \tag{52}$$

which is the net number of type (f) diagrams coming from the lowest order connected diagrams of U_4.

Thus far we have considered only those diagrams of U_4 which come from the connected diagrams present at three kernels. There are other diagrams which contribute to U_4. These are taken into account by considering certain types of disconnected diagrams which become connected upon the addition of more binary kernels. We note that no such diagrams occur in the case of b_3 because all diagrams containing two binary kernels are connected in the case of three particles.

At three binary kernels in U_4 there are 24 disconnected diagrams of the type (g) which transform as another binary kernel is added to give 72 type (n) and 48 type (m) diagrams. When this topological type was summed from connected diagrams, the diagrams

of type (n) were not included. These type (n) diagrams correspond to the Lee-Yang diagram of Figure 9 (a). These type (n) diagrams occur in U_4 as follows:

4 kernels	5 kernels	6 kernels	...
3(24)	$-(2)(3)24$ $-(3)^2 24$	$(2)^2(3)24$ $(2)(3)^2 24$ $(3)^3 24$	

This can be written as the sum

$$3(24)\sum_{n=0}^{\infty}(-1)^n\left[x^n + x^{n-1}y + \ldots + xy^{n-1} + y^n\right] = 6 \qquad (53)$$

which is the net number of type (n) diagrams arising from the 24 type (g) disconnected diagrams at three binary kernels.

At two binary kernels there are 24 type (h) diagrams which transform to give 24 type (p), 48 type (q), 24 type (r), and 24 type (s) diagrams. We included these types (q) and (r) when we counted the lowest order diagrams and included the type (s) as the type (g) considered above. We have not yet dealt with the 24 type (p) diagrams and must count all connected diagrams arising from adding binary kernels to them.

The 24 type (p) diagrams give rise to type (t) diagrams which we must count. The type (t) diagrams correspond to the diagram of Figure 9 (b). These enter as follows:

4 kernels	5 kernels	6 kernels	...
(2)24	-(2)24	+(2)24	
	$-(2)^2 24$	$+(2)^2 24$	
		$+(2)^3 24$	

and this may be expressed as the sum:

$$(2)(24)\left\{1 + (-1)\left[1 + 2\right] + \left[1 + (2)(1) + (2)^2\right] + \ldots\right\}$$

$$= (2)(24) \sum_{\substack{n=0 \\ x=1\ ;\ y=2}}^{\infty} (-1)^n \left[x^n + x^{n-1}y + \ldots + xy^{n-1} + y^n\right] \tag{54}$$

$$= (2)(24) \sum_{n_1=0}^{\infty} (-x)^{n_1} \sum_{n_2=0}^{\infty} (-y)^{n_2} = 8 \text{ [illegible]} \tag{55}$$

which is the number of type (t) diagrams coming from the disconnected (p) ones present at two kernels in U_4.

The type (p) diagrams also give rise to 24 type (u) diagrams which must be counted. Using the same analysis as for the type (t) diagrams we find four type (u) diagrams as the net contribution from disconnected diagrams.

The type (m) diagrams give a net contribution of -3 diagrams like type (n) when they are summed up.

Also present at two kernels are six type (i) diagrams which transform to give types (v) and (w). We have dealt with type (w) but (v) diagrams give rise to type (x) which have not been treated yet. These type (x) diagrams correspond to the diagram of Figure 9(c).

The (x) diagrams from this source can be summed up to give a net contribution of +4 type (x) diagrams to U_4.

The types (t), (u), and (x) which we have considered also transform to give diagrams like type (n). Without giving the details which are familiar from the treatment of these types which come from the connected diagrams, the type (n) diagrams coming from types (t) and (x) can be summed to give -6, and those coming from type (u) can be summed to give -3. This means we have a total of -6 diagrams of typological type (n) coming from disconnected diagrams.

Using this summation technique we find the number of type (d), (e), and (f) diagrams coming from disconnected diagrams. The results are tabulated in Table I. The values of the integral contributions of the six topological types of diagram contributing to b_4 have been determined.[10]

The result for b_4 is

$$b_4 = (\lambda^{-12}/4!)\left[-12 \sqcap \; -4 \nwarrow \; + 12 \nearrow \; + \quad 3 \square \; + \right.$$
$$\left. - 6 \boxslash \; + \quad 1 \boxtimes\right]$$

$$b_4 = -\lambda^{-12}\,(3.5539832\, b_o^{\,3})$$

which leads to the correct result for the fourth virial coefficient for classical hard spheres.

The analysis of b_3 and b_4 using the classical application of the Lee-Yang binary kernel technique is very cumbersome because of the necessity of summing the diagrams of all orders in the binary kernel to obtain the well-known classical results. Clearly this classical adaptation is not useful unless a convenient expansion

of the binary kernel (as was done by Lee and Yang[11] in treating the quantum mechanical system) can be found. Some further work corroborating this analysis has been published[12] since the appearance of reference 9. The use of an expansion for the binary kernel permitted a consideration of diagrams of order $l - 1$ and l only for each b_l in the limit of very low temperatures for the quantum mechanical system. Attempts to find an analogous expansion for use in classical applications were unsuccessful.

Chapter V

The Binary Kernel Expansion in the Classical Limit: the work of Pais and Uhlenbeck

Pais and Uhlenbeck[3] have studied the Lee-Yang binary kernel method and examined its relation to the Mayer expansion for classical systems. They show how the Lee-Yang quantum mechanical diagrams may be obtained by in their words "a process of blowing up" the Mayer graphs of classical theory by working backwards from the initial assumption that the Lee-Yang result is identical to the Mayer expansion in the classical limit. In Chapter IV we explicitly demonstrated this identity for the lowest b_ℓ values ($\ell = 2, 3, 4$) of the hard sphere potential. Their method is to consider each graph drawn for the classical system to be related to a sum over a class of Lee-Yang diagrams given for the quantum mechanical system. The first step in this development by Pais and Uhlenbeck is to draw the Mayer classical graphs for a given number of particles ℓ. Next, lines are drawn upward from the vertices of these graphs perpendicular to the planes of the graphs. These vertical lines form vertical planes between the vertices of the classical graphs. The quantum graphs are now obtained by "blowing up" the classical graphs. Blocks (represented by shaded areas) are placed in the vertical planes starting at the bottom. Each successive block must touch the top of the preceeding one as the blocks are added. A graph with at least one block in each vertical plane is said to be a connected

quantum graph. No two blocks may be placed in succession in the same vertical plane. The order in which the blocks are built up is significant. A quantum graph is associated with each classical Mayer graph by summing over all possible numbers of blocks which can occur. The blocks are closely related to the binary kernel operator. Pais and Uhlenbeck associate the k^{th} block in the vertical plane between particles i and j with the operator

$$C(\beta_k; ij) = B(\beta_k; ij)\, e^{-\beta_k \sum_{n'=1}' (p_{n'}^2/2m)} \tag{1}$$

where $B(\beta_k;ij)$ is the binary kernel operator defined by Lee and Yang

$$B(\beta_k; ij) = -V_{ij}\, e^{-\beta_k \left(\frac{p_i^2}{2m} + \frac{p_j^2}{2m}\right) + V_{ij}} \tag{2}$$

where V_{ij} is the potential energy of interaction of molecules i and j. The prime on the summation sign in the definition equation (1) means that $n' \neq i,j$. The $C(\beta_k;ij)$ operators occurring at the bottom of the quantum graph occur to the right of those representing blocks located higher up in the diagram when the operator for the diagram is written down. In the formulation of Pais and Uhlenbeck the operator

$$\int \cdots \int d\beta_1 \cdots d\beta_n \, e^{-(\beta - \sum_{i=1}^{n} \beta_i) T_\ell}$$

$$\times C(\beta_n; i_n j_n) C(\beta_{n-1}; i_{n-1} j_{n-1}) \cdots C(\beta_1; i_1 j_1) \tag{3}$$

is associated with the quantum graph of ℓ points with n blocks. Here T_ℓ is the kinetic energy of the particles

$$T_\ell = \sum_{k=1}^{\ell} (p_k^2/2m) \tag{4}$$

The domain of the β integration is restricted by the condition

$$\sum_{k=1}^{n} \beta_k \leq \beta \tag{5}$$

Pais and Uhlenbeck write the operator associated with each Mayer graph G as follows:

$$U_\ell(G) = e^{-\beta T_\ell} S \int \cdots \int d\beta_1 \cdots d\beta_N \, e^{T_\ell \sum_{k=1} \beta_k}$$

$$\times C(\beta_N; i_N j_N) \cdots C(\beta_1; i_1 j_1) \tag{6}$$

The round summation means: (1) summation over all numbers n(i,j) of blocks between all pairs of particles i,j occurring in the graph G from n(i,j) = 1 to ∞. The total number of blocks N is $N = \sum_{ij} n(i,j)$. (2) for given n(i,j) summation over all allowed permutations of the blocks. Permutations in which two blocks between the same two particles are immediately adjacent to one another are not allowed. The number of connected quantum graphs for given number of blocks n(i,j) between the various particles i,j in the graph is calculated by Pais and Uhlenbeck. This is the number of permitted arrangements in β space of the links present in the diagram.

It is pointed out by Uhlenbeck and Pais that the case of two particles is instructive for comparison between quantum theory and classical theory. The quantum graph in the case of two particles contains only one block and the quantum mechanical U_2 is expressed by Pais and Uhlenbeck as

$$U_2(1,2) = e^{-\beta T_2} \int_0^{\beta} d\beta_1 \, e^{+\beta_1 T_2} (-V_{12}) \, e^{-\beta_1 (T_2 + V_{12})} \tag{7}$$

This equation becomes valid for the classical system if the kinetic and potential energies are allowed to commute:

$$U_2^{\,c} = e^{-\beta T_2} f_{12} \tag{8}$$

where

$$f_{ij} = e^{-\beta V_{ij}} - 1 \tag{9}$$

is the Mayer f_{ij} function.

Pais and Uhlenbeck prove that the binary kernel expansion converges to the Mayer expansion for classical systems in the classical limit. This is done by first assuming that for a given U_ℓ the classical result, equal to a product of Mayer f_{ij} functions (specified for that U_ℓ) multiplied by $e^{-\beta T_\ell}$ would be obtained in the classical limit from the quantum mechanical formulation. This assumption directly implies a general formula for the number of arrangements in β space for the links in a Lee-Yang diagram containing a specified number of links (binary kernels) operating between the pairs of particles in the diagram. The results of this formula agree with the number of arrangements obtained by direct counting in the classical case. This proves the convergence to the classical result of the quantum mechanical binary kernel expansion in the classical limit.

A simple example of this convergence is given by Pais and Uhlenbeck as shown in equations (7) and (8) above where the quantum mechanical formulation of U_2 involving only one quantum graph converges to the classical result when the kinetic and potential energies are allowed to commute. For all cases where $\ell \geq 3$ the binary kernel expansion for b_ℓ is a sum of an infinite number of graphs

resulting from the operation of an infinite number of binary kernels. This complicates the situation for systems of three or more particles. Pais and Uhlenbeck deal with this general case using the classical limit of their quantum mechanical formulation given above as equation (6). The restriction on the domain of the integration specified in equation (5) is replaced in equation (6) as follows

$$U_{\ell}(G) = e^{-\beta T_{\ell}} (1/2\pi i) \int_{-i\infty}^{+i\infty} \frac{e^{\ell t}}{t} dt \int_0^{\infty} \cdots \int_0^{\infty} d\beta_1 \cdots d\beta_N$$
$$e^{(T_{\ell} - t) \sum_{k=1}^{N} \beta_k} C(\beta_N; i_N j_N) \cdots C(\beta_1; i_1 j_1) \tag{10}$$

where the path of the t-integration is from $-i\infty$ to $+i\infty$ in the t-plane and to the right of all singularities in t of the integrand. This replacement allows the limits on the β-integrations to be from zero to ∞. Substituting the definition given in equations (1) and (2) of the operator $C(\beta_k; i,j)$ gives

$$U_{\ell}(G) = e^{-\beta T_{\ell}} (1/2\pi i) \int_{-i\infty}^{+i\infty} \frac{e^{\ell t}}{t} dt \int_0^{\infty} \cdots \int_0^{\ell} d\beta_1 \cdots d\beta_N$$
$$\times e^{(T_{\ell} - t) \sum_{k=1}^{N} \beta_k} (-V_{i_N j_N}) e^{-\beta_N \sum_{n'=1}^{\ell} (p_{n'}^2/2m)} e^{-\beta_N V_{i_N j_N}}$$
$$\times (-V_{i_{N-1} j_{N-1}}) e^{-\beta_{N-1} \sum_{n'=1}^{\ell} (p_{n'}^2/2m)} e^{-\beta_{N-1} V_{i_{N-1} j_{N-1}}} \cdots$$
$$\times \cdots (-V_{i_1 j_1}) e^{\beta_1 \sum_{n'=1}^{\ell} (p_{n'}^2/2m)} e^{-\beta_1 V_{i_1 j_1}} \tag{11}$$

In the classical limit the kinetic and potential energies are allowed to commute:

$$U_\ell (G)^c = e^{-\beta T_\ell} (1/2\pi i) \int_{-i\infty}^{+i\infty} \frac{e^{\xi t}}{t} dt \int_0^\infty \cdots \int_0^\infty d\beta_1 \cdots d\beta_N$$

$$\times e^{-t \sum_{k=1}^{N} \beta_k} (-V_{i_N j_N}) e^{-\beta_N V_{i_N j_N}} (-V_{i_{N-1} j_{N-1}})$$

$$e^{-\beta_{N-1} V_{i_{N-1} j_{N-1}}} \cdots (-V_{i_1 j_1}) e^{-\beta_1 V_{i_1 j_1}} \qquad (12)$$

Performing the integrations over the β's results in

$$U_\ell (G)^c = e^{-\beta T_\ell} (1/2\pi i) \int_{-i\infty}^{+i\infty} \frac{e^{+\beta t}}{t} dt \, S \left[\frac{V_{i_N j_N}}{t + V_{i_N j_N}} \right]$$

$$\times \left[\frac{V_{i_{N-1} j_{N-1}}}{t + V_{i_{N-1} j_{N-1}}} \right] \cdots \left[\frac{V_{i_1 j_1}}{t + V_{i_1 j_1}} \right] \qquad (13)$$

The pairs of particles in the classical Mayer graph $U_\ell (G)^c$ are $i_1 j_1$, $i_2 j_2$ ... , $i_m j_m$. The round summation S means summation over all numbers of blocks $n(i_1 j_1)$, $n(i_2 j_2)$, ... , $n(i_m j_m)$ which can occur between the pairs of particles $n(i_1 j_1) = 1$ to ∞,..., $n(i_m j_m) = 1$ to ∞ . The total number of blocks N is given by

$$N = \sum_{i<j} n(i,j) \qquad (14)$$

also for each $n(i_1j_1)$, ... $n(i_mj_m)$ a summation must be made over all allowed permutations of the blocks. Some permutations are not permitted because two blocks between the same pair of particles cannot be immediately adjacent to one another. In the quantum graph the order in which the blocks are built up is important. In the classical limit this order is not significant because each allowed permutation of the blocks contributes the same product of factors to $U_{\ell}(G)^c$. Each of these products of binary kernel factors is weighted according to the number of allowed permutations for it. In the method of Pais and Uhlenbeck in the classical limit the round summation is replaced by a summation over all numbers of blocks occurring $n(i_1j_1)$, $n(i_2j_2)$, ... , $n(i_mj_m)$ between the particles each summand weighted by the weighting factor

$$\chi\left[n(i_1j_1),\ n(i_2j_2),\ \ldots,\ n(i_mj_m)\right] =$$

$$\chi\,(n_1,\ n_2,\ \ldots,\ n_m) \tag{15}$$

The absolute value of $\chi(n_1,\ n_2,\ \ldots\ ,\ n_m)$ gives the number of allowed arrangements in ϱ space for $n(i_1,j_1)$ kernels linking particles i_1,j_1; $n(i_2,j_2)$ kernels linking i_2,j_2, ... $n(i_m,j_m)$ kernels linking i_m,j_m. The function $\chi(n_1,n_2,\ \ldots\ n_m)$ will be positive or negative in sign depending on the total number of binary kernels occurring because each binary kernel or block occurs as the factor $-V_{ij}e^{-\varrho_k V_{ij}}$ for k^{th} block between particles i and j. This gives for $U_{\ell}(G)^c$ from equation (13) the

result

$$U_\ell (G)^c = e^{-\beta T_\ell} \sum_{n_1=1}^{\infty} \sum_{n_2=1}^{\infty} \cdots \sum_{n_m=1}^{\infty} \chi(n_1, n_2, \ldots, n_m)$$

$$\times (1/2\pi i) \int_{-i\infty}^{+i\infty} \frac{e^{\beta t}}{t} dt \prod_{\lambda=1}^{m} \left[\frac{-V_{i_\lambda j_\lambda}}{t + V_{i_\lambda j_\lambda}} \right]^{n(i_\lambda, j_\lambda)} \tag{16}$$

the definition of $U_\ell (G)^c$ is

$$U_\ell (G)^c = e^{-\beta T_\ell} \prod_{\lambda=1}^{m} f_{i_\lambda j_\lambda} \tag{17}$$

Assuming this should hold in (16) we have

$$f_{i_1 j_1} \cdots f_{i_m j_m} = \sum_{n_1=1}^{\infty} \sum_{n_2=1}^{\infty} \cdots \sum_{n_m=1}^{\infty} \chi(n_1, n_2, \ldots, n_m)$$

$$\times (1/2\pi i) \int_{-i\infty}^{+i\infty} \frac{e^{\beta t}}{t} dt \prod_{\lambda=1}^{m} \left[\frac{-V_{i_\lambda j_\lambda}}{t + V_{i_\lambda j_\lambda}} \right]^{n(i_\lambda j_\lambda)} \tag{18}$$

Pais and Uhlenbeck use the identity

$$\prod_{\lambda} f_{i_\lambda j_\lambda} = \prod_{\lambda=1}^{m} (e^{-\beta x_\lambda} - 1) = (1/2\pi i) \int_{-i\infty}^{+i\infty} \frac{e^{\beta t}}{t}\, dt$$

$$\times \left[(-1)^m + (-1)^{m-1} \sum_{\lambda} \frac{t}{t_1 + x_\lambda} + \right.$$

$$\left. + (-1)^{m-2} \sum_{\lambda>\mu} \frac{t}{t + x_\lambda + x_\mu} + \ldots + \frac{t}{t + x_1 + x_2 + \ldots + x_m} \right] \tag{19}$$

in equation (17) to find

$$\chi(n_1, n_2, \ldots, n_m) = \int_0^\infty dz\, e^{-z} \prod_{\lambda=1}^{m} L_{n_\lambda}^{(-1)}(z) \tag{20}$$

where $L_n^{(-1)}(z)$ is an associated Laguerre polynomial defined by

$$L_n^{(-1)}(z) = \sum_{k=1}^{n} (-1)^k (z^k/k!) \binom{n-1}{n-k} \tag{21}$$

Some examples of results for $\chi(n_1, n_2, \ldots, n_m)$ are

$\chi(1,1,1) = -6$ Corresponding to six Δ figures at 3 kernels

$\chi(2,2,2) = 30$ Corresponding to the thirty $\Delta\!\!\!\Delta$ figures of the 90 Δ integrals at 6 kernels

$\chi(2,1,1) = 6$ Corresponding to $\frac{1}{3}$ of the $\Delta\!\!\!\Delta$ figures at 4 kernels (three ways to choose pairs for repeated kernel)

These results for $\chi(n_1, n_2, \ldots, n_m)$ are thus in agreement with the number of arrangements in $\mathcal{C}$ space obtained by direct counting from the Lee-Yang diagrams in the classical case. Thus Pais and Uhlenbeck have proved that the Lee-Yang binary kernel expansion converges in the classical limit to the Mayer expansion for classical systems.

Chapter VI

Attempts to Obtain Quantum Mechanical Corrections to the High Temperature Third Virial Coefficient of Hard Spheres Using the Binary Kernel Expansion

The third virial coefficient C is related to the fugacity coefficients b_2 and b_3 by

$$C = (2N^2/\lambda^{-6})\ (2b_2^{\,2} - \frac{b_3}{\lambda^{-3}}) \tag{1}$$

The possibility of using the Pais-Uhlenbeck formulation[3] of the binary kernel expansion to calculate quantum mechanical corrections to the third virial coefficient was part of this study. The second fugacity coefficient b_2 is obtained by integration of U_2 over the coordinates of the two particles. The binary kernel expansion form for b_2 involves only one block (or binary kernel) acting between the two particles and therefore is not an infinite sum. To calculate b_3 we must "blow up" in the sense of Pais and Uhlenbeck the classical Mayer graphs of Figure 10. The binary kernel expansion for one of these involving only two lines may be written in the classical limit according to Pais and Uhlenbeck[3]

$$U_3' = e^{-\beta T_3}\ (1/2\pi i) \int_{-i\infty}^{+i\infty} \frac{e^{\beta t}}{t}\, dt \sum_{n_1=1}^{\infty} \sum_{n_2=2}^{\infty} \chi(n_1,n_2) z_1^{n_1} z_2^{n_2} \tag{2}$$

In this notation U_3' refers to the contribution of this one type of diagram of U_3 to U_3. Also

$$T_3 = (p_1^2/2m) + (p_2^2/2m) + (p_3^2/2m) \tag{3}$$

$$z_1 = \frac{X_1}{X_1 + t} \tag{4}$$

$$z_2 = \frac{X_2}{X_2 + t} \tag{5}$$

where X_1 and X_2 are for example V_{12} and V_{13} respectively. In equation (2) n_i is the number of binary kernels between the i^{th} pair of particles and the function $\chi(n_1, n_2, \ldots, n_m)$ without sign gives the number of arrangements of the kernels such that kernels between the same two particles are not nearest neighbors. Since the z_i are taken as positive $\chi(n_1, n_2, \ldots, n_m)$ will have the sign $(-1)^{n_1 + n_2 + \ldots n_m}$ because in the classical limit each β integration produces a factor

$$\frac{-X_i}{X_i + t} \tag{6}$$

The function $\chi(n_1, n_2, \ldots, n_m)$ has been calculated by Pais and Uhlenbeck[3]

$$\chi(n_1, n_2, \ldots, n_m) = \int_0^\infty ds\, e^{-s} L_{n_1}^{(-1)}(s)\, L_{n_2}^{(-1)}(s) \ldots L_{n_m}^{(-1)}(s) \tag{7}$$

where the associated Laguerre polynomial is defined by

$$L_n^{(-1)}(s) = \sum_{k=1}^{n} (-1)^k \frac{s^k}{k!} \binom{n-1}{n-k} \tag{8}$$

Using equation (7) in equation (2) we have

$$U_3' = e^{-\beta T_3} (1/2\pi i) \int_{-i\infty}^{+i\infty} \frac{e^{\beta t}}{t} dt \sum_{n_1=1}^{\infty} \sum_{n_2=1}^{\infty}$$

$$\times \int_0^{\infty} ds\, e^{-s} z_1^{n_1} L_{n_1}^{(-1)}(s)\, z_2^{n_2} L_{n_2}^{(-1)}(s) \tag{9}$$

making use of the property of the associated Laguerre polynomials given by

$$\sum_{n=1}^{\infty} z^n L_n^{(-1)}(s) = \left[e^{-s(z/1-z)} - 1 \right] \tag{10}$$

the summations over the infinite number of kernels acting in (9) can be written

$$U_3' = e^{-\beta T_3}\,(1/2\pi i)\int_{-i\infty}^{+i\infty}\frac{e^{\beta t}}{t}\,dt\int_0^{\infty}ds\,e^{-s}\left[e^{-s(z_1/1-z_1)}-1\right]$$

$$\times\left[e^{-s(z_2/1-z_2)}-1\right] \tag{11}$$

$$U_3' = e^{-\beta T_3}\,(1/2\pi i)\int_{-i\infty}^{+i\infty}\frac{e^{\beta t}}{t}\,dt\left[\frac{z_1z_2(2-z_1-z_2)}{1-z_1z_2}\right] \tag{12}$$

In this same way we may write for the Mayer triangle diagram of U_3:

$$U_3'' = e^{-\beta T_3}\,(1/2\pi i)\int_{-i\infty}^{+i\infty}dt\left[\frac{(1-z_1)(1-z_2)(1-z_3)}{1-z_1z_2-z_1z_3-z_2z_3+2z_1z_2z_3}+\right.$$

$$-\frac{(1-z_1)(1-z_2)}{1-z_1z_2}-\frac{(1-z_1)(1-z_3)}{1-z_1z_3}-\frac{(1-z_2)(1-z_3)}{1-z_2z_3}$$

$$\left.+(1-z_1)+(1-z_2)+(1-z_3)-1\right] \tag{13}$$

If the z_i have the classical limiting forms as given in equations (4) and (5) the complex integration on t in (12) and (13) will result in the respective classical product of Mayer f_{ij} functions for each of these two types of diagrams of U_3.

We have attempted to modify the z_i so as to include quantum mechanical corrections. The z_i function has the form of the common factor arising from each independent ξ_i integration as was pointed out in connection with the expression (6). The binary kernel expansion for U_2 involves only one block between the two particles and therefore only one z_i factor is involved. The quantum mechanical corrections to the second virial coefficient for the case where the symmetry of the wave functions need not be considered ($\lambda < \sigma$) giving the "direct" second virial coefficient direct have been determined for the system of hard spheres at high temperature

$$B_{2_{direct}} = B_2^C \left[1 + (3/2\sqrt{2})(\lambda/\sigma) + (1/\pi)(\lambda/\sigma)^2 + \right.$$

$$+ (1/16\pi\sqrt{2})(\lambda/\sigma)^3 - (1/105\pi^2)(\lambda/\sigma)^4$$

$$\left. + (1/640\pi^2\sqrt{2})(\lambda/\sigma)^5 + \ldots \right] \qquad (14)$$

where B_2^C is the classical second virial coefficient.

$$B_2^C = (2\pi N \sigma^3/3) \qquad (15)$$

The term in (λ/σ) was obtained by Uhlenbeck and Beth.[13] The term in $(\lambda/\sigma)^2$ apart from a missing factor of two was obtained by Mohling.[14] The correct term $(1/\pi)(\lambda/\sigma)^2$ was first given by Handelsmann and Keller who also obtained the term in

$(\lambda/\sigma)^3$.[15] The term in $(\lambda/\sigma)^4$ was obtained by Hemmer and Mork.[16] The last term was obtained by Hill.[17]

The second virial coefficient is related to b_2 by

$$B_2 = \frac{-Nb_2}{\lambda - 6} \tag{16}$$

In the development of Pais and Uhlenbeck the case of U_2 is instructive for comparison between classical theory and quantum theory.[3] We have

$$U_2 = e^{-\beta T_2} \int_0^{\beta} d\beta_1 \, e^{+\beta_1 T_2} (-V_{12}) e^{-\beta_1 (T_2 + V_{12})} \tag{17}$$

In the classical limit the kinetic and potential energies commute to give

$$U_2 \longrightarrow U_2^{C} = e^{-\beta T_2} f_{12} \tag{18}$$

The form for U_2 containing quantum corrections is

$$U_2^{qu} = e^{-\beta T_2} f_{12} (1 + d_1 \beta^{1/2} + d_2 \beta + d_3 \beta^{3/2} + \\ + d_4 \beta^2 + d_5 \beta^{5/2} + \ldots) \tag{19}$$

The coefficients d_1 to d_5 are the coefficients of the respective powers of $\beta = \left(\frac{1}{kT}\right)$ in the quantum correction terms of B_2 direct as given in equation (14) such that

$$d_1 = (h/2\pi m)(3/2\sqrt{2}\,\sigma)$$

$$d_2 = (h^2/2\pi m)(1/\pi\,\sigma^2)$$

$$d_3 = \frac{h^3}{(2\pi m)^{3/2}} \left(\frac{1}{16\pi\sqrt{2}\,\sigma^3}\right) \tag{20}$$

$$d_4 = (-h^4/2\pi m^2)(1/105\pi^2\sigma^4)$$

$$d_5 = \frac{h^5}{(2\pi m)^{5/2}} \left(\frac{1}{640\pi^2\sqrt{2}\,\sigma^5}\right)$$

In order to incorporate the quantum mechanical corrections we have focused on the single β integration in equation (17) which gives rise to the Mayer f_{12} function of (18). We write

$$U_2^{qu} = e^{-\beta T_2} \int_0^{\beta} (-V_{12}) e^{-\beta V_{12}} \left\{1 + d_1 \beta_1^{1/2} + d_2 \beta_1 + d_3 \beta_1^{3/2} + \right. \\ + d_4 \beta_1^2 + d_5 \beta_1^{5/2} + \ldots + \left[\frac{e^{-V_{12}} - 1}{V_{12}}\right]\left[(1/2) d_1 \beta_1^{1/2} \right. \\ \left. \left. + d_2 + (3/2) d_3 \beta_1^{1/2} + 2 d_4 \beta_1 + (5/2) d_5 \beta_1^{3/2}\right]\right\} \tag{21}$$

where the factor enclosed in the brackets on the right side of equation (21) is present because of the lack of commutability of the kinetic and potential energies in the quantum case.

In order to modify the z_i factor arising from each integration in the Pais-Uhlenbeck formulation of the binary kernel expansion we have used (21) to write (not including terms beyond d_2)

$$U_2 = e^{-\beta T_2}(1/2\pi i)\int_{-i\infty}^{+i\infty}\frac{e^{\beta t}}{t}\,dt\int_0^{\beta} d\beta_1(-X_1)e^{-\beta_1(X_1+t)}$$

$$\left\{1 + d_1\beta_1^{1/2} + d_2\beta_1 + \ldots + \frac{(e^{-\beta_1 X_1} - 1)}{X_1}\left(-\frac{1}{2}d_1\beta_1^{-1/2} + \right.\right.$$

$$\left.\left. + d_2 + \ldots + \right)\right\} \tag{22}$$

where $X_1 = V_{12}$. After integrating over β_1 we obtain

$$U_2^{qu} = e^{-\beta T_2}(1/2\pi i)\int_{-i\infty}^{+i\infty}\frac{e^{\beta t}}{t}\,dt\left\{\left[\frac{X_1}{X_1+t}\right]\left[e^{-\beta(X_1+t)} - 1\right]\right.$$

$$+ d_1\left[\left(\frac{-X_1}{(X_1+t)^{3/2}}\right)N\left(\sqrt{\beta(X_1+t)}\right) + \left(\frac{X_1}{X_1+t}\right)\beta^{1/2}e^{-\beta(X_1+t)}\right.$$

$$\left. - \left(\frac{1}{t^{1/2}}\right)N(\sqrt{\beta t}) + \left(\frac{1}{(X_1+t)^{1/2}}\right)N\left(\sqrt{\beta(X_1+t)}\right)\right] +$$

$$+ d_2\left[\left(\frac{X_1}{X_1+t}\right)\beta e^{-\beta(X_1+t)} + \frac{X_1}{(X_1+t)^2}\left(e^{-\beta(X_1+t)} - 1\right)\right.$$

$$\left.\left. - \frac{1}{X_1+t}\left(e^{-\beta(X_1+t)} - 1\right) + \frac{1}{t}\left(e^{-\beta t} - 1\right)\right]\right\} \tag{23}$$

where

$$\int_0^{\sqrt{\beta}} e^{-x_1\beta_1} = (1/\sqrt{x_1})N(\sqrt{\beta x_1}) \tag{24}$$

so that

$$\int_0^{\beta} \sqrt{\beta_1}\, e^{-\beta_1 x_1}\, d\beta_1 = \frac{1}{x_1^{3/2}} N(\sqrt{\beta x_1}) - \frac{\beta^{1/2} e^{-\beta x_1}}{x_1} \tag{25}$$

We also write

$$E(\sqrt{\beta Q'}) = \frac{N(\sqrt{\beta Q'})}{\sqrt{\beta Q'}} \tag{26}$$

Then

$$z_1 = \left(\frac{-X_1}{X_1 + t}\right) f(X_1 + t) - d_1 \left[\left(\frac{-X_1}{X_1 + t}\right)\beta^{1/2} E\left(\sqrt{\beta (X_1 + t)}\right) + \left(\frac{X_1}{X_1 + t}\right)\beta^{1/2} e^{-\beta(X_1 + t)} - \beta^{1/2} E(\sqrt{\beta t}) + \beta^{1/2} E\left(\sqrt{\beta(X_1 + t)}\right)\right] - d_2 \left[\left(\frac{X_1}{X_1 + t}\right)\beta\, e^{\beta(X_1 + t)} + \left(\frac{X_1}{(X_1 + t)^2}\right) f(X_1 + t) - \left(\frac{1}{X_1 + t}\right) f(X_1 + t) + \left(\frac{1}{t}\right) f(t)\right] \tag{27}$$

where

$$f(\alpha) = e^{-\beta\alpha} - 1 \tag{28}$$

and (-1) has been factored out because the sign is to be included in $\chi(n_1, n_2, \ldots, n_m)$.

That the z_1 containing quantum corrections defined by equation (27) does give the correction form for U_2^{qu} is shown by using it in the Pais-Uhlenbeck formulation for U_2 as follows

$$U_2 = e^{-\beta T_2} (1/2\pi i) \int_{-i\infty}^{+i\infty} dt \frac{e^{\beta t}}{t} z_1 \tag{29}$$

Performing the integration on the complex variable t results in

$$U_2^{qu} = -e^{-\beta T_2} (e^{-\beta X_1} - 1)(d_1 \beta^{1/2} + d_2 \beta + \ldots) \tag{30}$$

Integrating this over the coordinates and momenta we obtain the correct form for b_2 containing the first two quantum correction terms which leads to the correct result for $B_{2\,direct}$, the second virial coefficient including the first two quantum correction terms.

The general form for the first quantum correction term to all virial coefficients for a ν-dimensional hard sphere gas at high temperature has been given by Hemmer.[18] General first quantum

corrections to all virial coefficients for three dimensional hard sphere systems at high temperatures have also been given by Jancovici.[19] Jancovici has also found the second quantum correction to the third virial coefficient for hard spheres at high temperatures.[20]

Application of the z_i from equation (27) in equations (12) and (13) which are the summation of the contributions of the two topological types of diagram contributing to b_3 does not lead to the correct quantum corrections in b_3. Therefore use of the z_i in these equations does not check the results of Hemmer and Jancovici for the quantum corrections to the third virial coefficient and our formulation of the z_i is a sufficient but not necessary form to yield quantum corrections when used in the Pais-Uhlenbeck form of the binary kernel expansion.

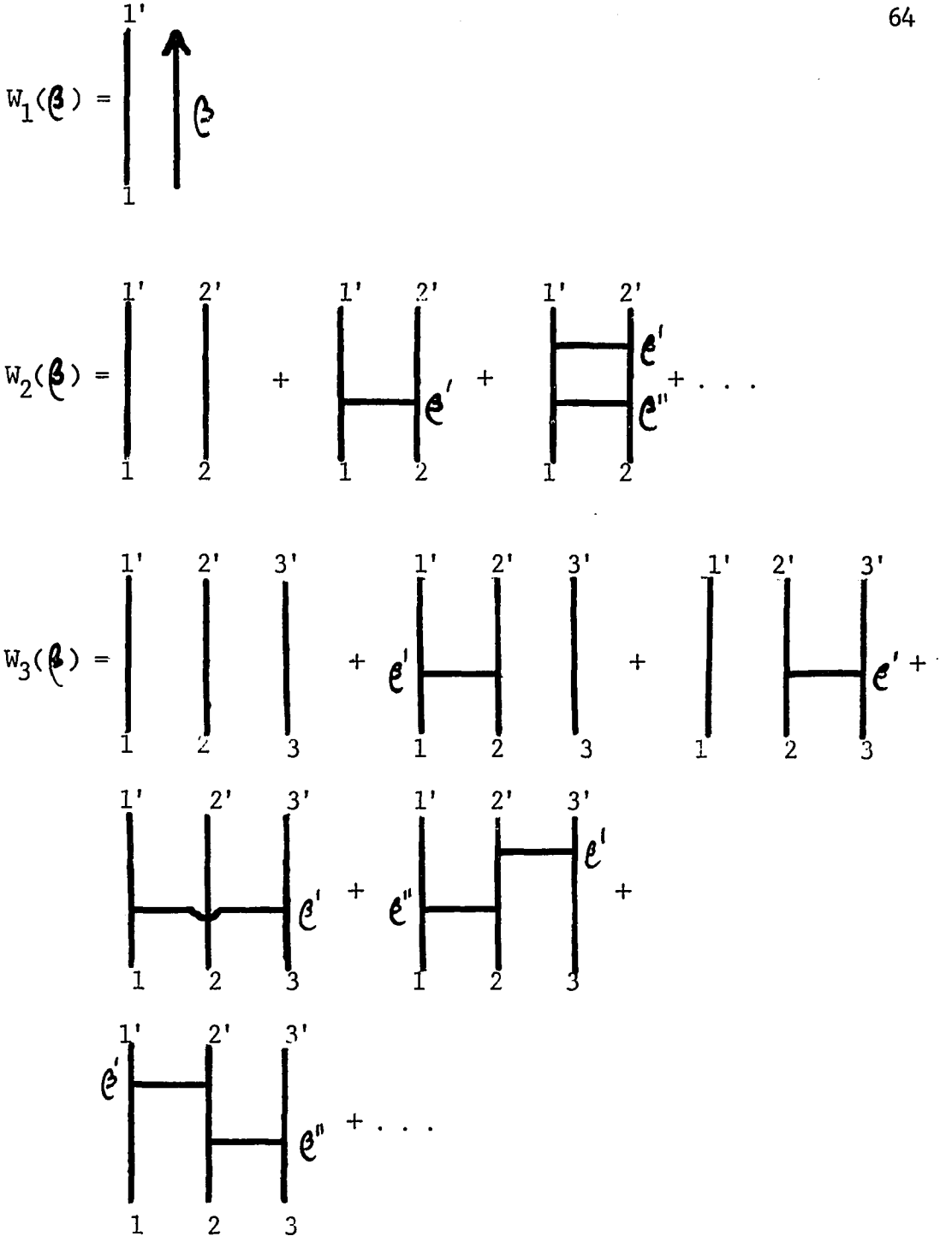

Figure 1. Examples of Lee-Yang Diagrams which Represent Operators for a One-particle, Two-particle, and Three-particle System.

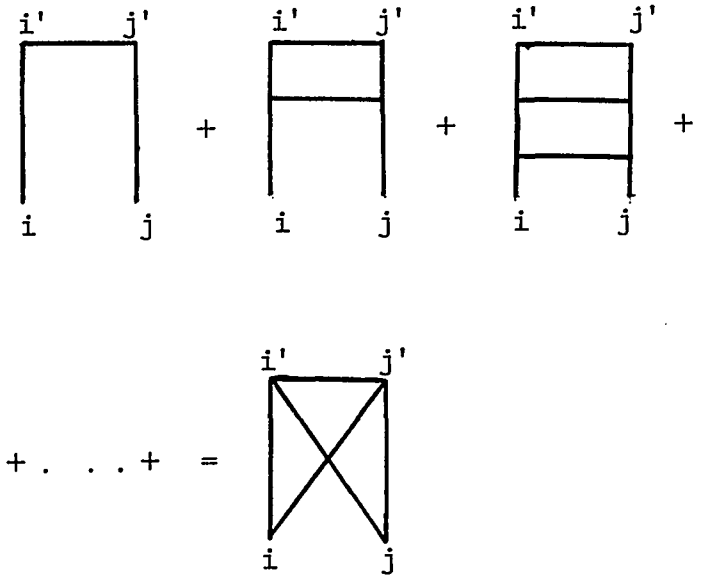

Figure 2. Diagramatic Representation of the Binary Kernel.

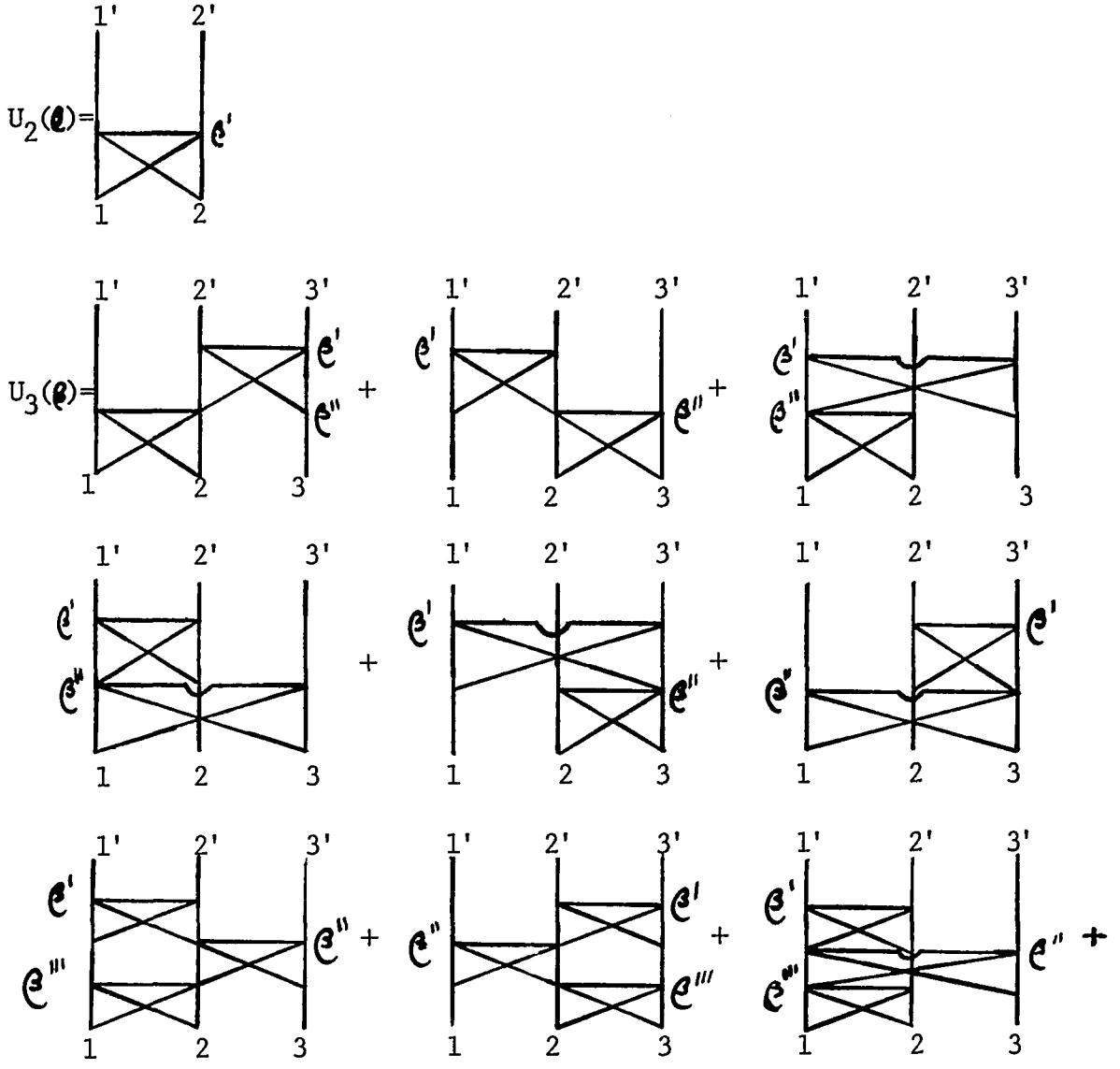

Figure 3. Diagrams Representing $U_2(\mathcal{E})$ and $U_3(\mathcal{E})$ in Terms of the Binary Kernel.

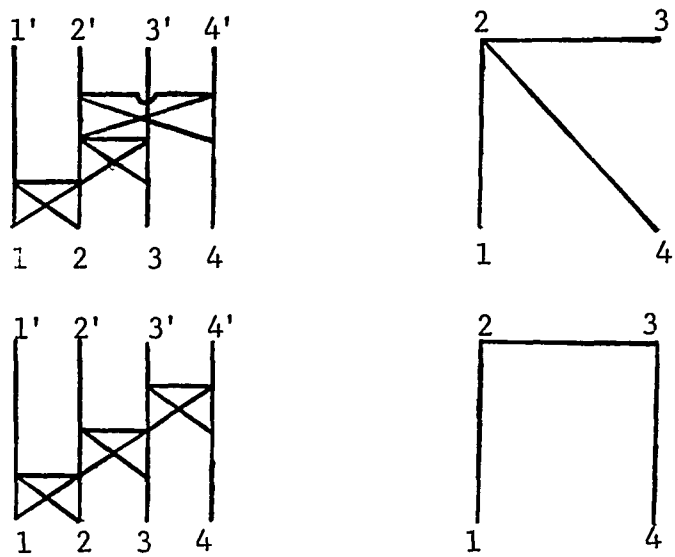

Figure 4. Correspondence Between Lowest Order Diagrams and Tree Skeletons.

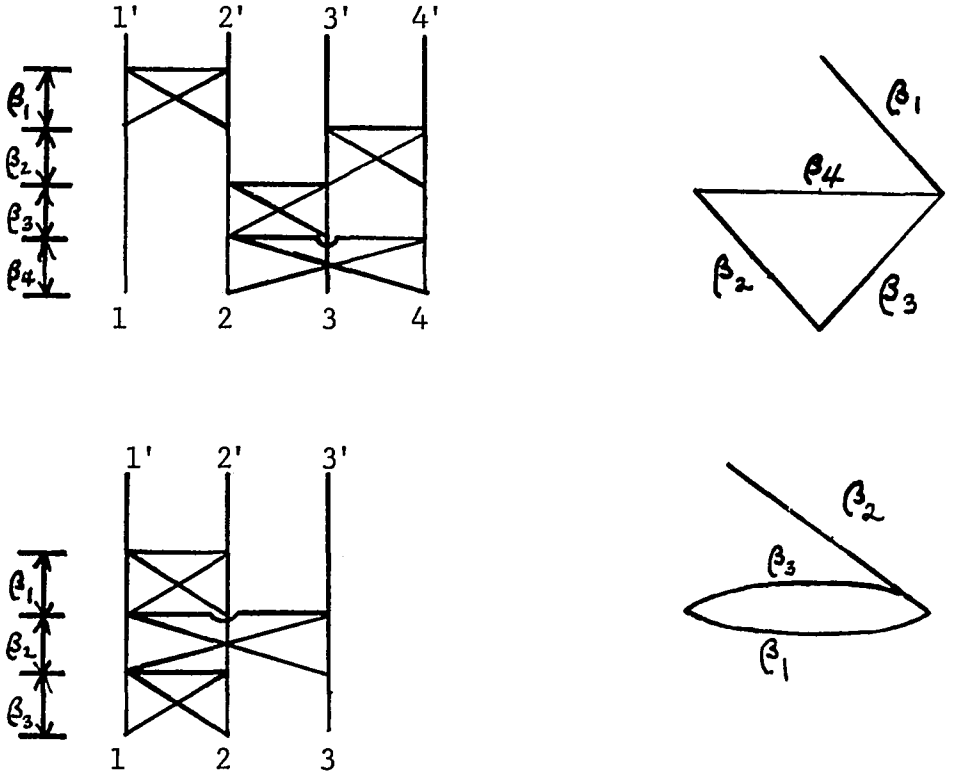

Figure 5. Lee-Yang Diagrams and Their Skeletons.

When $\mu = 3$ the loop is a triangle. When $\mu = 2$ no such polygon is found but the single link joining two particles is repeated. For the diagrams above in which $\mu = 2$ switching of the β_3 with β_1 does not generate a new skeleton.

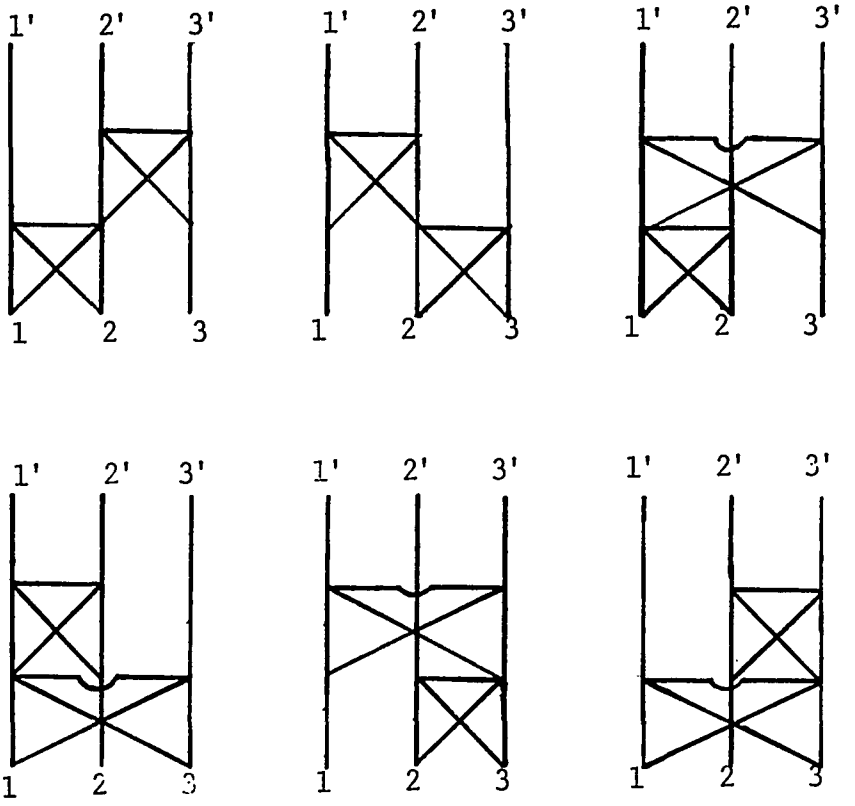

Figure 6. The Six Lowest Order Diagrams of U_3.

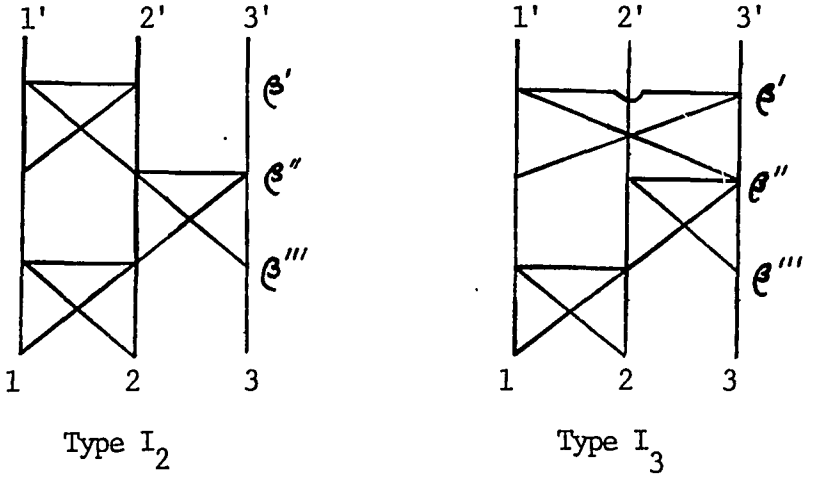

Figure 7. The Two Topological Types of Next-to-lowest Order Diagrams of U_3. The interactions in type I_2 involve only two of the three possible links, while type I_3 has all three links involved in its interactions.

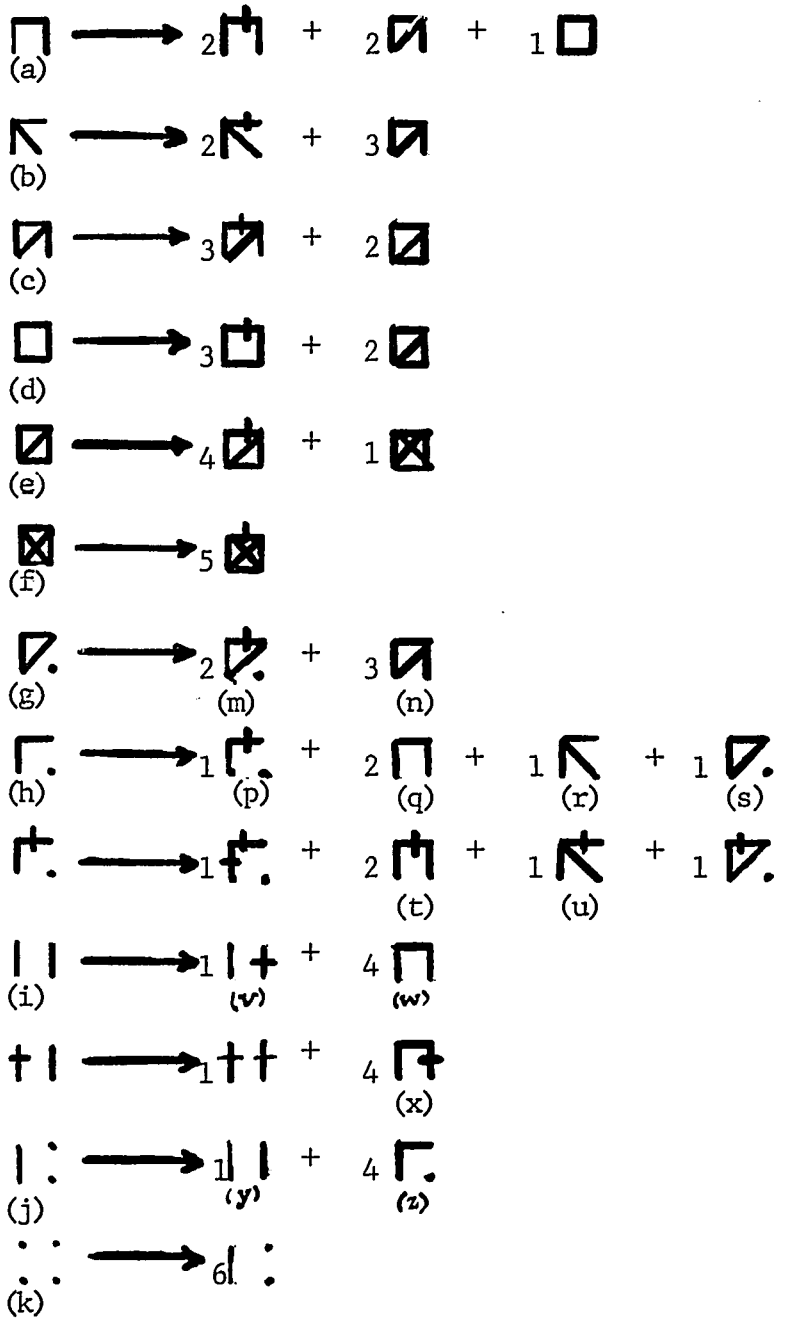

Figure 8. The Transformation Properties of the Binary Kernel Diagrams in the Four-particle Case for Hard Spheres. The arrow stands for "upon adding another link gives". The cross marks in certain diagrams indicate repeated links which do not change the absolute value of the integrals.

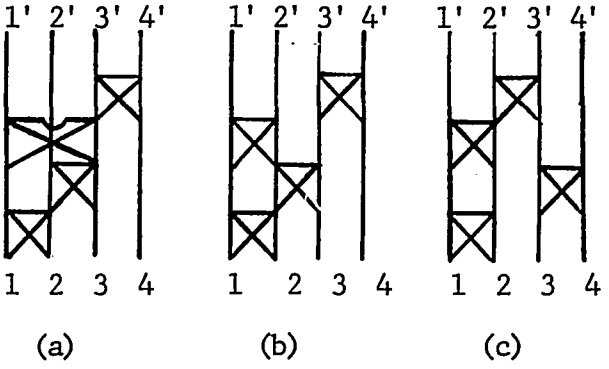

Figure 9. Diagrams Representative of Those which Come from Disconnected Diagrams as a Result of Adding the Topmost Binary Kernel.

Table I

A Summary of the Diagrams Contributing to b_4

The number of diagrams coming from the 96 lowest order diagrams and from the disconnected diagrams which contain two and three binary kernels are given. Column 1 gives the sum on diagrams arising from connected lowest order diagrams. Column two gives the sum on diagrams arising from disconnected diagrams which become connected in higher order. Column three gives the total integral contribution multiplied by λ^{+12}. $b_0 = (2\pi\sigma^3/3)$

Column 1	Column 2	Column 3
-8	+4	$-4(2b_0)^3$
-24	+12	$-12(2b_0)^3$
+18	-6	$+12(15b_0^2/8)(2b_0)$
+6	-3	$+3(272b_0^3/105)$
$\frac{-48}{5}$	$\frac{+18}{5}$	$-6(6347b_0^3/3360)$
$\frac{+8}{5}$	$\frac{-3}{5}$	$+1.2669040b_0^3$

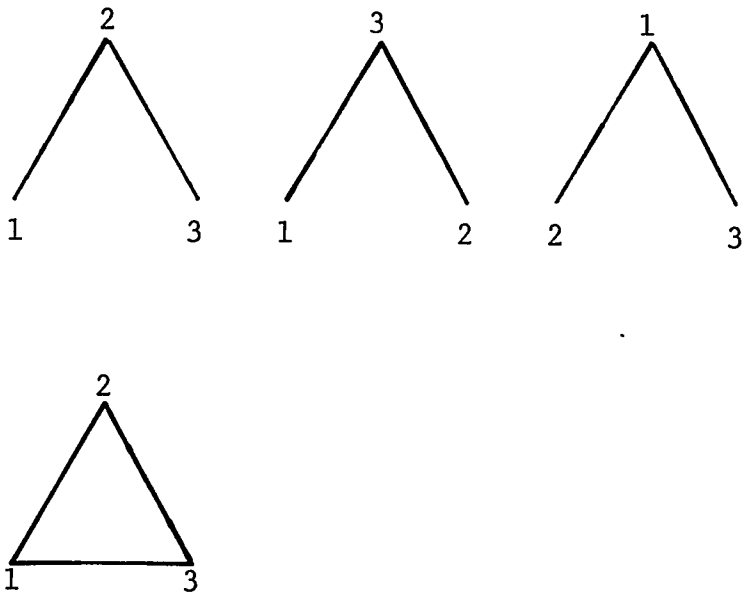

Figure 10. The Classical Mayer Graphs for Three Particles.

References

1. T.D. Lee and C.N. Yang, Phys. Rev. 113, 1165 (1959).
2. Ibid., 117, 12 (1960).
3. A. Pais and G.E. Uhlenbeck, Phys. Rev. 116, 250 (1959).
4. H.D. Ursell, Proc. Cambridge Phil. Soc. 23, 685 (1927).
5. Joseph E. Mayer and Maria Goeppert Mayer, Statistical Mechanics, John Wiley and Sons Inc., New York, 1940, pp. 277-294.
6. B. Kahn and G.E. Uhlenbeck, Physica 5, 399 (1938).
7. G. Polya, Acta. Math. 68, 145 (1937).
8. J. Moon, in Graph Theory and Theoretical Physics, ed. by F. Harary, Academic Press, New York, 1967, p. 264.
9. C.E. Hecht and J. Lind, Phys. Rev. A 1, 952 (1970).
10. J.S. Rowlinson, Proc. Roy. Soc. (London) A279, 147 (1964).
11. T.D. Lee and C.N. Yang, Phys. Rev. 116, 25 (1959).
12. W.G. Gibson, Phys. Rev. A 4, 2108 (1971).
13. G.E. Uhlenbeck and E. Beth, Physica 3, 729 (1936).
14. F. Mohling, Phys. Fluids 6, 1097 (1963).
15. R.A. Handelsmann and J.B. Keller, Phys. Rev. 148, 94 (1966).
16. P.C. Hemmer and K.J. Mork, Phys. Rev. 158, 114 (1967).
17. R.N. Hill, J. Math. Phys. 9, 1534 (1968).
18. P.C. Hemmer, Phys. Letters 27A, 377 (1968).
19. B. Jancovici, Phys. Rev. 178, 295 (1969).
20. Ibid., 184, 119 (1969).